Scientific Reports

https://doi.org/10.1038/s41598-026-43248-7

Article in Press

# Neuroinflammatory crosstalk between microglia and astrocytes increases viral replication in an iPSC-derived model of CNS HIV infection

Received: 19 September 2025

Accepted: 3 March 2026

Published online: 11 March 2026

Cite this article as: Gesualdi J., Prah J., Solomon S. *et al.* Neuroinflammatory crosstalk between microglia and astrocytes increases viral replication in an iPSC-derived model of CNS HIV infection. *Sci Rep* (2026). https://doi.org/10.1038/s41598-026-43248-7

James Gesualdi, Jude Prah, Shiden Solomon, Jayden Cyrus, Ernesto Baçi, Peter J Gaskill, Çagla Akay-Espinoza & Kelly L. Jordan-Sciutto

**Title:**
Neuroinflammatory crosstalk between microglia and astrocytes increases viral replication in an iPSC-derived model of CNS HIV infection

**Authors:**
James Gesualdi[1], Jude Prah[2], Shiden Solomon[3], Jayden Cyrus[3], Ernesto Baçi[5], Peter J Gaskill[6], Çagla Akay-Espinoza[3], Kelly L. Jordan-Sciutto[3] (corresponding author, jordank@upenn.edu)

1: University of Pennsylvania, Perelman School of Medicine, Philadelphia, PA, US
2: Novartis (US), Boston, MA, US
3: University of Pennsylvania, School of Dental Medicine, Philadelphia, PA, US
4: Brown University, Department of Molecular Biology, Cell Biology, and Biochemistry, Providence, RI, US
5**:** University of Pennsylvania, School of Arts and Sciences, Philadelphia, PA, US
6: Drexel University, Department of Pharmacology and Physiology, Philadelphia, PA, US

**Abstract:**
People living with HIV suffer multiple comorbid conditions related to chronic inflammation at increased rates compared to the general population, even when on effective antiretroviral therapy. In particular, current data indicate that the increased incidence and severity of neurocognitive impairment (NCI) are associated with unresolved neuroinflammation. Attempts to treat NCI in people living with HIV by reducing inflammation have thus far been unsuccessful, suggesting that a more mechanistic understanding of inflammatory processes in the CNS during HIV is necessary. Here, we use iPSC-derived microglia (iMg) and astrocytes (iAst) to model HIV infection in the CNS. We show that our iMg robustly express markers associated with microglial identity and are susceptible to HIV infection, but exhibit lower HIV replication rates and weaker immune response to HIV challenge compared to monocyte-derived macrophages. Coculture of iAst with iMg leads to a much stronger pro-inflammatory immune response, and, surprisingly, a robust increase in rates of HIV replication. Increased replication in iMg/iAst cocultures is associated with higher levels of multiple pro-inflammatory cytokines, including TNF✔, which is produced by iAst upon exposure to HIV-infected iMg. Addition of exogenous TNF✔ to iMg during HIV infection is also sufficient to increase rates of replication, and neutralization of TNF✔ via adalimumab/Humira treatment in iMg/iAst cocultures reduces replication. Blocking NF-kB signaling with iKK inhibitor Bay-11-7082 (Bay-11) demonstrates that increased HIV replication in iMg/iAst cocultures is due to increased NF-kB activity. Finally, we show that in HIV-infected iMg there is movement of lysosomes to the periphery of the cell membrane and release of lysosomal content into the extracellular space, suggesting that this dysregulated lysosomal flux could further contribute to

the pro-inflammatory microenvironment. We propose that this altered lysosomal trafficking and increased cytokine production drives a pro-inflammatory phenotype in glia and represents a potential source of unresolved neuroinflammation in people living with HIV.

**Acronyms and abbreviations used in this manuscript:**
HIV (Human Immunodeficiency virus), neurocognitive impairment (NCI), HIV-Associated neurocognitive disorder (HAND), HIV-associated brain injury (HABI), People living with HIV (PLWH), Anti-retroviral therapy (ART), Central nervous system (CNS) cerebrospinal fluid (CSF), Induced pluripotent stem cells (iPSCs), iPSC-derived microglia (iMg), iPSC-derived astrocytes (iAst), coculture (CC), conditioned media (CM), monocyte-derived macrophages (MDM), common myeloid progenitor (CMP).

## Introduction:

Approximately 40 million people worldwide are currently living with HIV. Since the advent of anti-retroviral therapy (ART), progression to acquired immunodeficiency syndrome (AIDS) has greatly declined[1]. Most people living with HIV (PLWH) on ART successfully achieve viral suppression if their treatment is not interrupted, eventually reaching a state in which viral RNA is undetectable in peripheral blood and transmission is not possible[2]. Indeed, PLWH on ART now have a lifespan nearly comparable to people without HIV[1,3]. Despite this remarkable progress, PLWH remain at increased risk for multiple chronic noncommunicable comorbidities, with heart disease, cancer, and cognitive decline being more likely to impact PLWH at earlier ages[4, 5]. Symptoms of neurocognitive impairment (NCI) are especially prevalent in PLWH once they reach the age of 50[4]. NCI represents a significant unmet challenge because roughly 50% of PLWH on ART develop some level of NCI or are diagnosed with HIV-associated neurocognitive disorder (HAND)[6, 7].

HAND is a spectrum of cognitive, behavioral, and motor deficits of varying severity that are often observed in PLWH. Viral contributions to neuropathology that lead to these deficits are referred to as HIV-associated brain injury (HABI)[8]. Importantly, HABI and associated symptoms of NCI tend to persist despite suppressive ART[9]. Persistent NCI in the context of suppressed viremia reduces quality of life for PLWH and therefore necessitates a deeper mechanistic understanding of the underlying pathological processes in the central nervous system (CNS).

Chronic inflammation is a pathological hallmark common to the diseases and comorbidities associated with HIV[4, 10]. Increases in systemic TNF✔, IL-6, and IL-1🚲 in PLWH are associated with increased incidence of both end-organ damage[11] and HAND[9]. Further, various single nucleotide polymorphisms in coding exons of *TNF* have been shown to increase the risk of several NCI symptoms in PLWH[12]. Additionally, indicators of neuroinflammation in the

cerebrospinal fluid (CSF) such as increased levels of neopterin, CCL2, TNF✔, and IL-6 are associated with an increased severity of NCI in PLWH[13, 14]. Given this association of multiple pro-inflammatory species with increased incidence and severity of comorbid conditions in PLWH, numerous immunomodulatory therapies have been explored in attempts to resolve chronic inflammation and improve quality of life for these individuals with limited success[5, 15]. Therefore, a mechanistic model of sources of neuroinflammation in the context of HABI is essential to inform clinicians of ideal cellular targets for anti-inflammatory adjunctive therapies that may be capable of mitigating HIV-associated NCI.

The precise mechanism through which HIV first accesses the CNS is a subject of ongoing study[16, 17, 18] . However, it is clear that myeloid cells in the CNS, including microglia and border-associated macrophages, begin harboring HIV shortly after initial infection[19] and typically before seroconversion[20]. This suggests that myeloid cells in the CNS serves as a viral reservoir for HIV in virtually all cases[21]. In the CNS, resident macrophages and microglia express CD4, CCR5, and CXCR4, and are the primary targets for HIV infection[22]. Even in the presence of suppressive ART, low level viral transcription and downstream neuroinflammation can occur in PLWH, and increased persistence of HIV transcription is associated with increased severity of NCI[20, 23, 24, 25]. Interestingly, the extent of neuroinflammation and neurotoxicity in PLWH on ART often exceeds the degree of pathology that can be explained by the modest levels of viral infection and HIV gene expression observed in the CNS. Indeed, recent transcriptomic studies of ex-vivo microglia isolated from PLWH on ART have shown that only roughly 0.5% of microglia harbor viral RNA transcripts[26]. This indicates that ongoing neuroinflammation and injury occur in the absence of direct viral-induced damage. In other words, there must exist mechanisms that contribute to tissue damage in the CNS that are at least somewhat independent of ongoing productive viral replication. These findings have prompted multiple studies on the role that bystander cells such as astrocytes may play in the context of HAND and HIV NCI.

Astrocytes, the most numerous cell type in the CNS, perform many critical neurotrophic functions under homeostatic conditions[27]. Additionally, astrocytes act to maintain the integrity of the blood brain barrier and contribute to immune responses to potential infectious challenges in the CNS[27]. Some studies suggest that astrocytes are capable of harboring HIV infection[28, 29], but evidence of active viral replication in astrocytes is limited and this remains an area of active debate[2028, 29, 30]. However, evidence of reactive or gliotic phenotypes among astrocytes is a common pathologic hallmark of many neuroinflammatory and neurodegenerative conditions and is associated with more severe NCI in PLWH[20, 31, 32], highlighting the role for astrocytes in HABI.

Studying the immune response of both microglia and astrocytes during HIV infection of the CNS at the mechanistic level has been challenging due to the

difficult nature of obtaining and culturing microglia *in vitro* without incurring broad loss of their *in vivo* characteristics[33]. Here, we use a coculture model of induced-pluripotent stem cell (iPSC)-derived microglia like cells (iMg) and astrocytes (iAst) to study the immune dynamics and crosstalk between these two glial populations in the context of HIV infection. We show that iMg express critical markers of microglial lineage and function and are susceptible to HIV infection with the patient-isolated strain HIV-1 ADA ($HIV_{ADA}$). We also demonstrate that HIV is capable of evading various canonical anti-viral immune responses in iMg and, surprisingly, that the coculture of iAst with HIV-infected iMg robustly increases the rate of viral replication. Our analyses reveal that this phenotype in cocultures is associated with the presence of pro-inflammatory cytokines produced by iAst, which in turn drive NF-kB activation in iMg, accelerating viral replication. Targeting pro-inflammatory cytokine production via neutralizing antibody blockade or attenuating NF-kB signaling via small molecule inhibition significantly reduces HIV replication rates observed in the iMg/iAst coculture model. Finally, we demonstrate that HIV infection in iMg leads to repositioning of lysosomes to the cell periphery and to increased exocytosis of lysosomal content into the extracellular space. This process suggests a potential microglia-dependent mechanism through which iAst become gliotic and begin producing TNF✓ and other pro-inflammatory molecules, driving the increased HIV replication observed in cocultures. Our findings provide a mechanistic foundation for the contribution of neuroinflammation to HABI in PLWH and suggest potential therapeutic avenues for reducing unresolved pathologic inflammation despite effective ART.

## Materials and Methods:

*Reagents*

Reagents used in these studies are depicted in Table 1 below.

**Table 1.** Reagents used in these studies

| Reagent | Source / Cat. |
|---|---|
| Human iPSC-Derived Astrocytes | Fujifilm / R1092 |
| Human IL-34 | PeproTech / 200-34 |
| Human TGF-🚲1 | PeproTech / 100-21 |
| Human MCSF | PeproTech / 300-25 |
| B-27 Supplement | ThermoFisher / 12587010 |
| Anti IBA-1 Antibody | Wako / 019-19741 |
| Anti GFAP Antibody | ThermoFisher / 13-0300 |
| Anti LAMP1 Antibody | Abcam / ab25245 |
| SNA-Cy3 | Vector Laboratories / CL-1303-1 |
| Anti NF-kB p65 Antibody | Cell Signal / D14E12 |
| VectaShield Mounting Medium | Vector Laboratories / H-1700 |

| | |
|---|---|
| Anti-TNF ✔ Antibody (Adalimumab / Humira) | Millipore Sigma / A-166 |
| Recombinant Human TNF ✔ | PeproTech / 300-01A |
| iKK Inhibitor (Bay-11) | Selleckchem / S2913 |
| HIV p24 Alphalisa | Revvity / AL291C |
| Human TNF ✔ Alphalisa | Revvity / AL3157C |
| Luminex 48-Plex Cytokine Kit | Bio-Rad / 12007283 |
| Cathepsin B ELISA Kit | Abcam / ab272205 |

*Differentiation iMg and monocyte-derived macrophages*

Human pluripotent stem cells derived from the skin fibroblasts of healthy adult donors were differentiated into common myeloid progenitors (CMPs), as previously described[34, 35]. In all experiments, CMPs were purchased from the Human Pluripotent Stem Cell Core at the Children's Hospital of Philadelphia, which serves as the honest broker and ensures that the lines are completely de-identified from the original donors. As such, there are no human subjects associated with these studies. CMPs were cultured in RPMI (HyClone) containing 10% FBS containing penicillin/streptomycin with 100 ng/mL IL-34, 50 ng/mL transforming growth factor beta TGFβ, and 25 ng/mL macrophage colony stimulating factor (MCSF) for 11 days to complete differentiation into iMg, as previously described[36]. CMPs were plated at a density of $5 \times 10^5$ cells /mL for all experiments, either in 24 or 96-well glass-like polymer coated culture plates (Cellvis). For immunostaining on glass coverslips, CMPs were plated and differentiated at the same density in 24 well glass-like polymer coated plates with circular coverslip inserts.

Monocyte-derived macrophages (MDMs) were differentiated from peripheral blood monocytes isolated from healthy volunteers using magnetic bead-based separation carried out by the University of Pennsylvania Human Immunology Core, as previously described[37]. Monocytes were plated at $5 \times 10^5$ cells /mL and differentiated in DMEM (Thermo Fisher) containing 10% FBS with penicillin/streptomycin and 20 ng/mL granulocyte-macrophage colony-stimulating factor for seven days, as previously described[37].

The University of Pennsylvania Human Immunology core maintains the IRB-approved protocol and the individual core users' receipt of these cells is considered secondary use of de-identified human specimens which is not considered human use by both the NIH and the University of Pennsylvania IRB.

*iMg/iAst cocultures*

Fully differentiated iAst were obtained from Fujifilm[38]. For monocultures of iAst and cocultures of iMg/iAst, glass-like polymer coated culture plates (CellVis) were coated with 1.2 ng/mL laminin in phosphate-buffered saline (PBS) for 2h. iAst were collected in BrainPhys (Thermo Fisher) supplemented with B27

(Thermo Fisher) and plated at a density of $10^5$ cells/mL. For iMg/iAst cocultures, CMPs were plated at $5 \times 10^5$ cells / mL in wells containing $10^4$ iAst. iMg/iAst cocultures were maintained in iMg media containing 10% FBS, 1X penicillin/streptomycin with 100 ng/mL IL-34, 50 ng/mL TGFβ, and 25 ng/mL M-CSF in addition to B27.

*Adalimumab,* TNF✔*, and Bay-11 formulation*

Adalimumab (Millipore Sigma), recombinant human TNFα (PeproTech), and Bay-11 (Selleckchem) were formulated in anhydrous DMSO. Working stocks were diluted in sterile PBS before preparing media aliquots with appropriate drug concentrations for treatment of monocultures or cocultures during HIV infection.

*HIV Stocks*

HIV-1 Jago is a macrophage-tropic isolate derived from the CSF of a patient with HIV-associated dementia[39]. As previously described, stocks were prepared by infection of primary T-lymphocytes derived from peripheral blood of healthy volunteers at the University of Pennsylvania Center for AIDS Research virology core followed by harvesting of cell-free supernatants.

HIV-1 ADA ($HIV_{ADA}$) is a patient-derived R5 tropic isolate derived from patient blood[40]. As previously described, stocks were prepared via infection of human t4-lymphoblastoid CEM-SS cells followed by collection of cell-free supernatants when syncytia were observable in the infected cells[40].

Concentration of viral stocks was determined by quantifying the amount of p24 per mL using a high-sensitivity AlphaLISA detection kit (Revvity). For negative control samples, viral stocks were heat inactivated by boiling at 100°C for 10 minutes then cooled to room temperature as previously described[37].

*HIV infection*

For all experiments except RNA sequencing, fully differentiated iMg, MDMs, and iMg/iAst cocultures were treated with 1 ng/mL p24 $HIV_{ADA}$ for 24 hours. In all experiments, a heat inactivated (dI) viral stock was included as a mock infection. After 24 hours of incubation, excess virions were removed via three sequential 60% washes with RPMI – in which 60% of the volume of the infected well was aspirated and replaced with an equal volume of plain RPMI – on post-infection day 0 (PID 0). Supernatants were collected from cultures at 3, 6, 9, or 12 days post-infection (PID 3, 6, 9, or 12) for various analyses. Supernatant collection was accompanied by 50% media changes on infected cells. For experiments in which infected cultures were treated with adalimumab, recombinant TNFα, or Bay-11, the reagents were diluted to the indicated

concentrations in the appropriate media for each culture condition and used to replace the media after supernatant collection beginning on PID3. For immunostaining, at indicated timepoints, the cultures were fixed using 4% paraformaldehyde (Thermo Fisher) in PBS for 20 min at room temperature.

*RNA isolation and sequencing*

Fully differentiated iMg and MDM cultures were infected with 50 ng/mL p24 HIV-1 Jago, using a higher concentration of HIV to increase the number of infected cells as required for sequencing. Following supernatant collection on PID 12, MDM and iMg were lysed in wells using the RLT buffer (Qiagen RNeasy Mini Kit 74104), and pooled RNA was isolated according to manufacturer protocols. RNA purity and concentration were confirmed using Nanodrop, and Zymo RNA Clean & Concentrator-25 was used on any samples that did not pass initial quality control based on an absorbance of ≥ 2 at 260/280 nm and an absorbance of ≥1.8 at 260/230 nm, with minimum concentration of 50 ng/uL.

The remaining steps were performed by Azenta Life Sciences. Briefly, purified RNA was used for mRNA-enriched library preparation and sequencing via Illumina HiSeq, with an average read depth of $22 \times 10^6$ reads/sample. Reads were trimmed using Trimmomatic v.0.36 and mapped to the *Homo Sapiens* GRCh38 reference genome using STAR aligner v.2.5.2b. Next, in the R computing environment, raw gene counts were calculated using featureCounts from the Subread package v.1.5.2. Raw counts were read into edgeR v.4.4, and low counts below 1 counts/million were filtered out as unexpressed genes. Counts were then normalized as transcripts/million[41]. Significantly differentially expressed genes (DEGs) were defined as those with a log-fold change ≥ 1.0 and an adjusted p value of ≤ 0.05. DEGs were analyzed using the gene set enrichment analysis package GSVA v.3.2[42]. Raw data from the bulk RNA sequencing experiment are available at NCBI GEO (accession GSE143685).

*Quantification of HIV p24 and cytokines in culture supernatants*

Supernatants from monocultures of iMg, MDMs, iAst, and from cocultures of iMg/iAst were collected following HIV infection and various drug treatments at PID 3, 6, 9, or 12. Supernatants were analyzed in duplicate by AlphaLISA to determine the levels of HIV capsid protein p24 (Revvity AL291C) or TNFα (Revvity AL3157C), as previously described according to manufacturer's protocols[43]. Briefly, supernatants were incubated with an anti-target primary antibody conjugated to streptavidin and biotinylated fluorescent acceptor beads for 1 h at RT. Next, fluorescent donor beads were added to the samples, which were incubated for 30 minutes at RT. The fluorescence was quantified using an Envision Excite plate reader and raw data were interpolated using a

standard curve to quantify the concentration of target analytes. The limits of detection on these assays were 1.8 pg/mL (p24) and 1.41 pg/mL (TNFα).

For unbiased cytokine assays, supernatants were assayed in duplicate using the Bio-Plex Pro Human Cytokine Screening Panel, 48-Plex (Bio Rad #12007283) by the University of Pennsylvania Human Immunology Core. Raw pg/mL values were presented indicated in scatter plots and fold change normalized to negative control (iMg treated with dI HIV) were presented as heat maps.

*iAst Monoculture Treatments*

iAst monocultures were plated at $1 \times 10^4$ cells per well on 96-well glass-like polymer coated plates coated with 1.2 ng/mL laminin for 2h at 37°C. iAst were treated with either 50% conditioned media from HIV-infected iMg, 100 ng/mL lipopolysaccharide, 10 ng/mL IL-1ß, or 10 ng/mL $HIV_{ADA}$ for 24 h. Cytokine levels in collected supernatants were analyzed by Alphalisa, or Bio-Plex Pro Human Cytokine Screening Panel, 48-Plex. Following supernatant collection, cells were fixed using 4% paraformaldehyde in PBS for 20 min at room temperature for immunostaining.

*Immunofluorescence staining*

Cells were fixed in culture plates with 4% paraformaldehydein PBS for 20 min and washed with PBS and PBS containing 0.1% Tween-20 (PBS-t) (Thermo Fisher). Cells were then blocked and permeabilized with 1.0% BSA in PBS containing 0.1% Triton-X (Thermo Fisher) (PBS-Tx) for 30 min. Cells were then incubated overnight at 4°C with primary antibodies targeting cell-surface markers (IBA-1 or SNA for iMg, GFAP for iAst) and proteins of interest (LAMP1, NF-kB p65) at appropriate dilutions in blocking buffer. Cells were then incubated for 2 h at room temperature with fluorescently labeled secondary antibodies corresponding to appropriate antibody host isotypes (1:200) and 4´,6-diamidino-2-phenylindole, dihydrochloride (DAPI, 1:1000). Stained cells were washed with PBS and stored in PBS at 4°C until imaging. For iMg differentiated on glass coverslips, coverslips were removed from culture plates with forceps and then mounted on slides using 20uL of VectaShield antifade mounting medium.

Images were captured using a Keyence BZ-X710 widefield fluorescent microscope with a 20X objective using DAPI, FITC, and Cy3 filter cubes or Leica TCS SP8 STED Confocal with a 40X objective. Scale bars were applied using ImageJ annotation software. For LAMP1 images, lysosomes were quantified near the cell membrane by manually defining a region of interest within ten pixels of the cell membrane as indicated by IBA-1 staining and then measuring the strength of local LAMP1 staining by quantifying the average intensity of 488 staining. For NF-kB p65 quantification, regions of interest were

automatically selected via thresholding whole cells and nuclei of microglia as indicated by SNA and DAPI staining, respectively, and strength of local NF-kB p65 signal was calculated by measuring the intensity of Cy5 staining in the indicated regions of interest.

*Statistical analysis*

Bulk RNA sequencing included three MDM donors and three iMg lines. For supernatant analyses and immunostaining, two to three differentiations of two to four iMg lines were used, with data averaged across differentiations to ensure that the observed changes were biologically and technically consistent. Numbers of biological replicates for a given experiment are detailed in the figure legends. HIV p24 and cytokine analyses from culture supernatants were evaluated using two-way ANOVA or multiple paired t-tests to compare across culture conditions and treatments, depending on the experimental design. Image quantifications were analyzed via multiple paired t-tests. Cathepsin B release was tabulated as fold change compared to untreated iMg monocultures and analyzed via Mann Whitney test. Whenever possible, data are visualized as a 'SuperPlot' in which technical replicates –distinct differentiations of a specific donor-derived iPSC line – within a biological replicate – defined throughout this manuscript as donor-derived iPSC lines isolated from distinct individuals – are color coded hollow icons, and averages of the constitutive technical replicates for each biological replicate are overlayed as a solid-colored point[44]. ANOVA and t-tests are performed on biological replicates using Graphpad PRISM version 10.4.2.

**Results:**

*iMicroglia express canonical cell-surface markers and are susceptible to HIV infection*

In a previous study[35], iMg differentiated using this cytokine cocktail have been shown to successfully exhibit a ramified morphology (Figure 1a) and robustly express classic microglial lineage markers, including *AIF1*, *TMEM119*, *P2RY12*, *SALL1*, *SMAD4*, *PTPRC*, *ITGAM*, *TGFBR1*, and *TGRBR2*[45] (Figure 1b). We have also previously reported that these iMg exhibit synaptophagocytic function[36], replicating key *in vivo* characteristics of human microglia. iMg also expressed high levels of HIV-associated cell-surface receptors *CD4*, *CCR5*, and *CXCR4* (Supplementary Figure 1a). Accordingly, $HIV_{ADA}$ was capable of entry and active replication in iMg. As expected, replication rates in iMg are reduced compared to those observed in human MDMs, suggesting that microglia are a suboptimal cellular host for HIV replication (Figure 1c), despite being permissive to infection. This may be due to a reduced expression of the HIV coreceptor *CCR5* in iMg compared to the MDMs (Supplementary Figure 1a).

MDMs have been shown to produce a robust pro-inflammatory response, including inflammasome activation, following HIV infection[46, 47, 37]. Accordingly, we found that HIV-infected MDMs secreted pro-inflammatory cytokines, such as IL-1β, TNFα, and IL-6, viral restriction factors such as IFNα2, and multiple chemokines (Figure 1d). In contrast, iMg failed to secrete any of these pro-inflammatory molecules at significant rates following infection with HIV at either the protein or the mRNA level (Figure 1d, 1e), with the exception of IL-1β, which was observed only at the transcript level(Figure 1e) indicating that mature IL-1β cleavage and secretion was not occurring in HIV-infected iMg monocultures, indicating reduced canonical anti-viral and pro-inflammatory immune responses in iMg compared to MDMs.

*Coculture of iMg with iAst leads to increased rates of HIV replication*

Given the weak immune response of iMg following challenge with HIV, we hypothesized that including iAst in coculture would enable a more pronounced immune activation. Various groups have also shown that differentiating iMg in the presence of other neuronal cells produces a more functional microglia population with a morphology more akin to homeostatic ramification typically observed *in vivo*[48]. Similarly, our iMg adopted a more readily observable ramified morphology under homeostatic conditions when differentiated in the presence of iAst (Figure 2a).

Surprisingly, the coculture of iMg with iAst led to a significant increase in HIV replication. Presence of iAst in a 1:5 ratio with iMg led to HIV virion production an order of magnitude higher than that observed in infected iMg alone, as measured by p24 levels in culture supernatants (Figure 2b, 2c). Importantly, this difference was not observed due to HIV replication in iAst themselves, as p24 was not observed via immunostaining in iAst in cocultures (Fig 2b) and production of p24 did not occur to any appreciable level in iAst monocultures (Figure 2d). This finding suggested that iAst increased the rate of active HIV replication in iMg without acting as a direct cellular target for HIV in our model. We next profiled the immune response in iMg/iAst cocultures to identify potential differences associated with this increase in virion production.

*iAst adopt a pro-inflammatory disease-associated phenotype when exposed to HIV-infected iMicroglia*

Based on the impact of iAst on HIV replication rates in iMg, we evaluated the cytokine profile of HIV-infected iMg in the presence and absence of iAst. HIV-infected iMg in monocultures exhibited a modest immune response marked by the production of CCL2 and IL-8 (Figure 3a, 3b). In contrast, HIV-infected iMg cocultured with iAst showed significantly increased production of CCL2, VEGF, IL-6, and TNFα compared to HIV-infected iMg monocultures, suggesting a more robust pro-inflammatory immune response to viral challenge (Figure 3a -3c). Interestingly, IFNα2 was not significantly upregulated in iMg/iAst

cocultures compared to iMg monocultures, suggesting that the nature of the immune response produced by cocultures in response to HIV infection was more broadly pro-inflammatory rather than specifically anti-viral in nature.

Next, we measured cytokine production by iAst in monocultures exposed to conditioned media of the HIV-infected iMg to determine the pro-inflammatory molecules specifically produced by iAst (Figure 3a, 3d). The treatment of iAst with conditioned media from the HIV-infected iMg led to the production of TNFα, but not that of IL-6 (Figure 3d, Supplementary Figure 3a). This indicates that factors secreted from HIV-infected iMg were sufficient to drive astrogliosis and pro-inflammatory cytokine production in iAst. Indeed, exposure of iAst monocultures to the supernatants from HIV-infected iMg led to a pro-inflammatory phenotype in iAst that is similar to the disease-associated astrocyte state observed in several neuropathic conditions[49].

*Astrocyte derived TNFα increases HIV replication rates in iMicroglia via NF-kB activation*

TNFα has been shown to be sufficient to increase transcription of integrated HIV genomes in reservoir studies and is considered a stimulus capable of accelerating active rather than latent or transcriptionally silent HIV infection[50, 51, 52]. Indeed, TNFα was shown to be sufficient to trigger reactivation of transcriptionally silent HIV infection in a microglia-derived cell line[53]. As such, we hypothesized that iAst-derived TNFα led to an increase in HIV replication observed in iMg cocultured with iAst. We tested this via addition of exogenous recombinant TNF✔ to monocultures of iMg infected with HIV and antibody blockade of TNFα in infected iMg/iAst cocultures. As expected, recombinant TNFα was sufficient to significantly increase HIV replication rates in monocultures of iMg (Figure 4a). Conversely, the neutralization of TNFα in infected cocultures via adalimumab treatment significantly reduced HIV replication, but not to the level observed in untreated iMg monocultures (Figure 4b). This suggested that while TNFα could drive increased HIV replication, it is likely not the only pro-viral factor secreted by iAst that acts to promote HIV replication in iMg in our model.

We hypothesized that the mechanism through which TNFα augmented HIV replication was dependent of NF-kB nuclear translocation. TNFα is a known inducer of NF-kB signaling[54, 52], and numerous studies have shown that NF-kB nuclear translocation can lead to increased transcription of the integrated HIV genome[55, 53], thereby increasing viral replication. We tested this by treating HIV-infected iMg/iAst cocultures with the Bay-11-7082 (Bay-11), which binds and inhibits inhibitory kappa beta kinase (iKK), preventing the phosphorylation and subsequent nuclear translocation of NF-kB p65[56]. Bay-11 treatment at 10 μM abrogated the observed increase in viral replication in iMg/iAst cocultures, suggesting that NF-kB signaling is critical for HIV replication in iMg (Figure 4c). Importantly, treatment of infected iMg/iAst cocultures with 10 μM Bay-11

reduced HIV replication to levels comparable to those observed in untreated iMg monocultures, suggesting that NF-kB signaling is the main mechanism driving the observed increase in viral replication in iMg/iAst cocultures. Additionally, Bay-11 treatment also abrogated the observed increase in TNFα production detected in HIV-infected cocultures, suggesting that astrocytic production of TNFα in iMg/iAst cocultures also depends on NF-kB signaling. To confirm that Bay-11 treatment successfully inhibited NF-kB dependent transcriptional regulation, we stained HIV-infected iMg monocultures and iMg/iAst cocultures with for NF-kB p65 (Fig 4e-f). Robust nuclear translocation was observed in iMg treated with 100ng/mL LPS as a positive control, showing the efficacy of this experimental design. As expected, p65 signal remained largely cytosolic in uninfected iMg, and nuclear p65 staining was more intense in HIV-infected iMg/iAst cocultures compared to HIV-infected iMg monocultures. This increase in nuclear translocation of NF-kB p65 was inhibited to the level seen in HIV-infected iMg monocultures in the presence of Bay-11.

*HIV infection causes lysosomal exocytosis in iMicroglia*

Given the robust pro-inflammatory phenotype observed in iAst exposed to conditioned media from infected iMg (Figure 3b), we hypothesized that factors secreted by infected iMg following HIV infection caused reactive gliosis in iAst. A recent proteomic study of HIV-infected macrophages showed that infection led to exocytosis of lysosomes, creating a pro-inflammatory microenvironment[57] and a study of HIV infection in microglial cell lines demonstrated a similar mechanism[58]. Additionally, multiple HIV viral proteins have been shown to be sufficient to alter lysosomal position, pH, and function in various cell types[59, 60, 61].

Thus, we hypothesized that HIV infection in iMg would alter lysosomal distribution, leading to lysosomal exocytosis and reactivity in iAst. Indeed, monocultures of HIV-infected iMg have lysosomes more proximal to the plasma membrane as determined by LAMP1 immunostaining (Figure 5a, 5b). Additionally, supernatants from HIV-infected iMg monocultures and iMg/iAst cocultures both had increased extracellular levels of cathepsin B compared to uninfected controls, indicating the release of lysosomal content into the extracellular space following HIV infection (Figure 5c). Interestingly, both iMg monocultures and iMg/iAst cocultures showed substantial cathepsin B release upon treatment with heat-inactivated (dI) $HIV_{ADA}$, suggesting that residual viral protein or nucleic acids remaining in this formulation are sufficient to perturb lysosomal flux in glia (Supplementary Figure 5a). These data provide a mechanism through which HIV infection in iMg creates a pro-inflammatory micro-environment driving astrocytic reactivity.

**Discussion:**

We show that our iMg reliably model *in vivo* microglia, including canonical cell surface marker expression and morphology. iMg allow the modeling of HIV infection *in vitro* and show a reduced immune response to HIV compared to other cell types susceptible to HIV infection, as shown in other recent studies of iPSC-derived microglia[40]. We also demonstrate that coculture of iMg with iAst leads to robust increases in the rate of HIV replication. This increase in viral replication is associated with astrocytic production of pro-inflammatory cytokines, particularly TNF✔, which drive NF-kB signaling, in turn leading to greater rates of viral replication in iMg. We also show that iAst exposed to infected iMg or soluble factors produced by infected iMg develop a pro-inflammatory disease-associated phenotype. This astrocytic activation is associated with dysregulated lysosomal flux and increased lysosomal exocytosis from iMg following HIV infection as measured by cathepsin B release.

Recent studies on HIV infection in the CNS of PLWH on ART have shown that, while pathologic changes constitutive of HABI such as inflammation, synaptic damage, and white matter abnormalities may be somewhat widespread[62], productively infected leukocytes are quite rare in the CNS[63, 32, 28]. In fact, a recent study estimated that only roughly 0.5% of microglia actively transcribe viral RNAs, which indicates infection[26]. Despite the minimal presence of HIV virions in the CNS, neuroinflammation and HABI continue to worsen overtime, leading to the onset of or exacerbation of NCI[13, 64, 65, 32]. The persistence of pathology in the context of a relative lack of viral infection suggests triggers of damaging neuroinflammation and gliosis that persist independently of replication[26, 66]. Accordingly, our coculture system could be leveraged to study the neuropathogenic potential of individual viral RNAs or proteins.

Our data show that even microglia that are not actively transcribing HIV may still exhibit dysregulated lysosomal flux (Supplementary Figure 5a). This may create a pro-inflammatory microenvironment due to the exocytosis of undegraded cellular materials, leading to astrogliosis. This is a potential mechanism through which neuronal injury may continue to persist and perhaps worsen in the setting of suppressive ART. The incidence of dysregulated lysosomal flux in the CNS of PLWH has not been demonstrated via immunohistochemistry. However, studies on peripheral biomarkers in Alzheimer's Disease patients have shown increased levels of proteins associated with aberrant autophagy and lysosomal function such as cathepsin D in peripheral blood[67]. Given the abundance of studies demonstrating the ability of HIV accessory genes to alter lysosomal distribution and drive lysosomal exocytosis in various cell types[57, 60 59], we propose that this is one mechanism through which residual viral proteins in the CNS[66] contribute to persistence of neuroinflammation and neuronal damage despite suppressive ART.

Our cytokine multiplex analysis shows that, while iAst exposed to supernatants from HIV-infected iMg produce TNFα, this treatment is not sufficient to significantly induce the secretion of IL-6 by iAst (Supplementary Figure 3a). However, cocultures of HIV-infected iMg and iAst show a robust production of IL-6. iAst likely adopt a pro-inflammatory profile following exposure to HIV-infected iMg due to exposure to factors released from iMg such as cathepsin B and ATP following lysosomal exocytosis and begin secreting TNFα. In turn, iMg, which robustly express both TNFR-1 and TNFR-2 (Supplementary Figure 2b), respond to this signal by upregulating pro-inflammatory cytokine production, including IL-6 specifically, as TNFα can induce IL-6 production in various cell types[68, 69]. We speculate that this may be a mechanism through which these pro-inflammatory cytokines are produced at higher levels in PLWH, potentially contributing to damaging neuroinflammation and HABI[89, 13]. Importantly, this study is limited in that quantification of IL-6 and other cytokines is performed at PID 12, so earlier spikes in cytokine production would be missed by this paradigm. This will be addressed in future studies.

This pro-inflammatory signaling axis elucidated in our model has implications for various phenomena observed in PLWH. CSF viral escape, i.e., presence of detectable HIV RNA in the CSF despite suppressive ART with either undetectable or significantly reduced viral RNA in peripheral circulation, is observed in 5-15% of PLWH[20, 70]. Various explanations have been proposed for CSF viral escape, such as poor penetrance of ART drugs into the CNS, development of escape mutations that confer drug resistance to novel HIV strains, and suboptimal patient adherence to prescribed ART. Our results suggest another potential mechanism: dysregulated lysosomal trafficking in microglia harboring HIV leads to the activation of neighboring astrocytes into a reactive, cytokine-producing state. Subsequently, TNFα or other NF-kB activating cytokines produced by reactive astrocytes promote transcription from the integrated HIV genome, leading to viral replication. This may lead to a positive feedback loop as more microglia are infected and begin experiencing dysregulated lysosomal flux. Evidence for this potential mechanism also comes from recent studies reporting that CSF viral escape is associated with both increased neuroinflammation[71] and astrocytic activation[72]. Future studies, such as single-cell RNA sequencing of brain tissue of SIV-infected rhesus macaques and tissue samples from PLWH experiencing CSF viral escape, are warranted to confirm and further elucidate the role of microglial lysosomal distress, astrogliosis, and NF-kB signaling in HIV-infected microglia as a potential signaling axis contributing to the persistence of neuroinflammation and neuronal injury despite suppressive ART.

A recent study has shown that damaged neurons induce HIV expression in previously latently infected microglia[73], indicating a mechanism through which neuronal injury itself may lead to viral replication and inflammation, creating a positive feedback loop that in turn may worsen neuronal health and NCI[74]. Our data suggest a comparable mechanism through which reactive astrocytes

rather than damaged neurons modulate HIV replication dynamics in microglia, driving increased replication via production of pro-inflammatory cytokines such as TNFα. Therefore, in line with many previous studies, our findings support the potential therapeutic role of anti-inflammatory agents to mitigate the incidence and severity of HIV-associated NCI in PLWH. Treatments designed to target reactive astrocytes may prove to be more feasible than those aimed at the rare HIV-infected microglia in ART-suppressed individuals, as astrocytes are a much larger population in the CNS.

Finally, our data showing dysregulated lysosomal positioning following HIV infection in microglia and associated lysosomal exocytosis, indicated by an increase in extracellular cathepsin B, suggest that lysosomal release may be involved in the propagation of a neuroinflammatory cascade in PLWH either as a legacy effect produced during acute infection or as a result of residual viral protein levels or low-level viral replication that may continue to occur despite ART. Accordingly, small molecules that can reduce lysosomal exocytosis and associated inflammation, such as the cannabinoid receptor 2 agonist JWH-133[57], may be considered for adjunctive therapies to reduce HIV-associated NCI.

**Figure Legends:**

**Figure 1: iMicroglia express canonical cell-surface markers and are susceptible to HIV infection.** (a). iMicroglia at 11 days *in vitro* via brightfield (top, 10X) or confocal (63X, bottom) microscopy. (b). Expression of indicated microglial lineage genes in iMg at 11 DIV compared to expression in MDM in log transformed transcripts per million. (c). HIV replication in iMg compared to MDM as measured by levels of HIV capsid protein p24 via alphalisa following infection with 1 ng/mL $HIV_{ADA}$. Data are expressed as Mean and SEM of 2 – 3 biological replicates in duplicate. (d). Heatmap indicating relative levels of indicated cytokines and chemokines produced by HIV-infected MDM (left) or iMg (right) compared to mock-infected iMg (center) at the protein level, measured by BioRad Luminex panel. Significant upregulation of analytes compared to mock-infected iMg are annotated via triangles in individual cells. Data are condensed from 2(MDM) to 5 (iMg) biological replicates. (e). Expression of indicated cytokines in iMg with or without HIV infection with HIV Jago at 50 ng/mL at PID 12 in log transformed transcripts per million * = $p < 0.05$, *** = $p < 0.001$, **** = $p < 0.0001$. Multiple paired T-tests.

**Figure 2: Coculture of iMicroglia with iAstrocytes leads to increased rates of HIV infection.** (a). iMg cocultured with iAst at 11 days in vitro via brightfield (top, 10X) or widefield (bottom, 40X) microscopy. (b). Widefield image of iMg (top) or iMg/iAst (bottom) cocultures following infection with 1 ng/mL $HIV_{ADA}$ captured at 40X at PID12. (c). HIV replication rates measured by HIV capsid protein p24 in iMg monocultures (circles) or iMg/iAst coclutures (triangles) after infection with 1 ng/mL $HIV_{ADA}$. iMg lines derived from distinct

donors (eg biological replicates) are indicated by different colors, and averages + SEM of technical replicates within each of the 4 groups of biological replicates are indicated by the overlayed solid-colored points and error bars. iMg lines included in this experiment are WT6 (black), WT10 (red), WT15 (blue), and WT17 (green). (d). HIV replication rates measured by HIV capsid protein p24 in iMg monocultures (circles), iMg + iAst cocultures (triangles), iAst monocultures (inverted triangles) after infection with 1 ng/mL $HIV_{ADA}$ or 1 ng/mL heat inactivated (dI) HIV (x). iMg groups include data condensed from four biological replicates, iAst groups include data condensed from three technical replicates. * = $p < 0.05$, ** = $p < 0.01$, **** = $p < 0.0001$. Two-way ANOVA (c) or Multiple paired T-tests (d).

**Figure 3: iAstrocytes adopt a pro-inflammatory disease-associated phenotype when exposed to HIV-infected iMicroglia** (a). Heatmap indicating relative levels of indicated cytokines and chemokines secreted by HIV-infected iMg monocultures (iMg+HIV, center), iMg/iAst cocultures (CC+HIV, right), and monocultures of iAst exposed to supernatants from HIV-infected iMg (iAst+iMg HCM, left) measured by biorad Luminex assay. Infected groups were treated with 1 ng/mL $HIV_{ADA}$. Color indicates log fold change compared to negative control (iMg + dI). Significant up/downregulation of analytes compared to HIV-infected iMg monocultures are annotated via triangles in individual cells. Data are averaged from 3 (iAst) to 5 (iMg and coculture) biological replicates (b). Raw pg/mL values measured by biorad Luminex of indicated cytokines and chemokines produced by HIV-infected iMg monocultures (circles), HIV-infected iMg + iAst coclutures (triangles). Data include 5 biological replicates. (c). TNFα levels secreted by HIV-infected iMg and HIV-infected iMg/iAst cocultures measured by biorad Luminex assay. iMg lines derived from distinct donors (eg biological replicates) are indicated by different colors, and averages + SEM of technical replicates within each of the 4 groups of biological replicates are indicated by the overlayed solid-colored points and error bars. iMg lines included in this experiment are WT6 (black), WT10 (red), WT15 (blue), and WT17 (green). (d). TNFα production measured via alphalisa for monocultures of iAst treated for 24h with the indicated stimuli. Data include 5 biological replicates per group measured in duplicate. * = $p < 0.05$, *** = $p < 0.001$, **** = $p < 0.0001$. Multiple paired T-tests.

**Figure 4: Astrocyte derived TNFα increase HIV replication rates in iMg via NF-kB activation** (a). HIV replication rates measured by HIV capsid protein p24 in iMg monocultures following infection with 1 ng/mL $HIV_{ADA}$ and addition of recombinant TNF□ at indicated concentrations. iMg lines derived from distinct donors (eg biological replicates) are indicated by different colors, and averages + SEM of technical replicates within each of the 2 groups of biological replicates are indicated by the overlayed solid-colored points and error bars. iMg lines included in this experiment are WT10 (black), and WT17 (red). (b). HIV replication rates measured by HIV capsid protein p24 in iMg/iAst cocultures following infection with 1 ng/mL $HIV_{ADA}$ and addition of TNF□

neutralizing antibody adalimumab at indicated concentrations. iMg lines derived from distinct donors (eg biological replicates) are indicated by different colors, and averages + SEM of technical replicates within each of the 4 groups of biological replicates are indicated by the overlayed solid-colored points and error bars. iMg lines included in this experiment are WT6 (black), WT10 (red), WT15 (blue), and WT17 (green). (c). HIV replication rates measured by HIV capsid protein p24 in iMg/iAst cocultures following infection with 1 ng/mL $HIV_{ADA}$ and addition of iKK□ inhibitor Bay-11 at 10 μM. iMg lines derived from distinct donors (eg biological replicates) are indicated by different colors, and averages + SEM of technical replicates within each of the 4 groups of biological replicates are indicated by the overlayed solid-colored points and error bars. iMg lines included in this experiment are WT6 (black), WT10 (red), WT15 (blue), and WT17 (green). (d). TNF□ production as measured by alphalisa in HIV-infected iMg monocultures, iMg/iAst cocultures, and iMg/iAst cocultures treated with 10 μM Bay-11. iMg lines derived from distinct donors (eg biological replicates) are indicated by different colors, and averages + SEM of technical replicates within each of the 4 groups of biological replicates are indicated by the overlayed solid-colored points and error bars. iMg lines included in this experiment are WT6 (black), WT10 (red), WT15 (blue), and WT17 (green). (e). Widefield microscopy images of iMg or iMg/iAst cocultures following the indicated treatments. SNA is a lectin staining marking iMg cellular membranes in Red, GFAP shows iAst in Cyan, NF-kB p65 is indicated in green and DAPI in blue. All images captured at 40X. (f). Quantification of (e) via automatic quantification of p65 staining in nuclei subtracted from whole cell p65 staining. iMg lines derived from distinct donors (eg biological replicates) are indicated by different colors, and averages + SEM of technical replicates within each of the 2 groups of biological replicates are indicated by the overlayed solid-colored points and error bars. iMg lines included in this experiment are WT15 (black), and WT17 (red). * = $p < 0.05$, ** = $p < 0.01$, **** = $p < 0.0001$. Two-Way ANOVA (a – d), Multiple paired T-tests (f).

**Figure 5: HIV infection leads to lysosomal release by iMg** (a). IBA1 (red), LAMP1 (green), and DAPI (blue) staining in iMg infected with 1 ng/mL $HIV_{ADA}$ (left) or dI (right) captured at 40X via confocal microscopy. (b). Quantification of local LAMP1 Mean Fluorescence Intensity in (a). A 10 pixel-wide region of interest was manually drawn at the plasma membrane of each cell, and mean fluorescence intensity of LAMP1 staining was measured, indicating trafficking of lysosomes to the cell periphery. iMg lines derived from distinct donors (eg biological replicates) are indicated by different colors, and averages + SEM of technical replicates within each of the 2 groups of biological replicates are indicated by the overlayed solid-colored points and error bars. iMg lines included in this experiment are WT6 (black), and WT17 (red). Data are condensed from 3 (dI) to 6 (HIV) independent experiments. (c). Cathepsin B measured in culture supernatants from indicated groups at PID 12. Data are condensed from four biological replicates and plotted as fold-change vs the

negative control group, iMg + Veh. iMg lines derived from distinct donors (eg biological replicates) are indicated by different colors, and averages + SEM of technical replicates within each of the 4 groups of biological replicates are indicated by the overlayed solid-colored points and error bars. iMg lines included in this experiment are WT6 (black), WT10 (red), WT15 (blue), and WT17 (green). * = $p < 0.05$, **** = $p < 0.0001$. Multiple paired T-tests (b), Mann-Whitney test (c).

**Supplementary Figure 1:** (a). Expression of indicated HIV-entry related genes in iMg at 11 DIV compared to expression in MDM in log transformed transcripts per million (b). Heatmap indicating relative levels of indicated cytokines and chemokines produced by HIV-infected MDM (left) or iMg (middle left) compared to mock-infected iMg (middle right) or iMg treated with 100 ng/mL LPS (right) at the protein level. Data are condensed from 2(MDM) to 5 (iMg) biological replicates. **** = $p < 0.0001$. Multiple paired T-tests.

**Supplementary Figure 2:** (a). Expression of indicated TNF□ receptor genes in MDM and iMg with or without infection with HIV Jago at 50 ng/mL in log transformed transcripts per million. **** = $p < 0.0001$. Multiple paired T-tests.

**Supplementary Figure 3:** (a). Raw pg/mL values measured by biorad Luminex of IL-6 produced by HIV-infected iMg monocultures (circles), HIV-infected iMg + iAst coclutures (triangles), or iAst treated with conditioned media from HIV-infected iMg (inverted triangles). Data include 3 (iAst) or 5 (iMg, CC) biological replicates. (b). TNF□ levels measured by alphalisa in iMg monocultures or iMg/iAst cocultures treated with vehicle (PBS) or 100 ng LPS. iMg lines derived from distinct donors (eg biological replicates) are indicated by different colors, and averages + SEM of technical replicates within each of the 2 groups of biological replicates are indicated by the overlayed solid-colored points and error bars. iMg lines included in this experiment are WT15 (black), and WT17 (red). * = $p < 0.05$, *** = $p < 0.001$. Multiple paired T-tests(a), One-Way ANOVA(b).

**Supplementary Figure 4:** (a). Manual counts of nucleated IBA1-positive microglia per tile-scan via widefield microscopy at 40X in the indicated culture conditions. iMg lines derived from distinct donors (eg biological replicates) are indicated by different colors, and averages + SEM of technical replicates within each of the 4 groups of biological replicates are indicated by the overlayed solid-colored points and error bars. iMg lines included in this experiment are WT6 (black), WT10 (red), WT15 (blue), and WT17 (green). * = $p < 0.05$. Multiple paired T-tests.

**Supplementary Figure 5**: (a). Cathepsin B measured in culture supernatants from indicated groups at PID 12. Data are condensed from four biological replicates and plotted as fold-change vs the negative control group, iMg + Veh. iMg lines derived from distinct donors (eg biological replicates) are

indicated by different colors, and averages + SEM of technical replicates within each of the 4 groups of biological replicates are indicated by the overlayed solid-colored points and error bars. iMg lines included in this experiment are WT6 (black), WT10 (red), WT15 (blue), and WT17 (green). * = $p < 0.05$, **** = $p < 0.0001$. Mann-Whitney test.

**Acknowledgments:** We would like to thank all the members of the Gaskill lab and myeloid working group for invaluable discussion on the data. The authors thank Max Eldabbas, Emileigh Maddox, Tanishk Sinha, and Jiayi Shu of the Human Immunology Core at the Perelman School of Medicine at the University of Pennsylvania for assistance with isolation and differentiation of primary human monocytes. The HIC is supported in part by NIH P30 AI045008 and P30 CA016520. This publication was made possible through core services and support from the Penn Mental Health AIDS Research Center (PMHARC), an NIH-funded program (P30 MH 097488). The following reagent was obtained through the NIH HIV Reagent Program, NIAID, NIH: Monoclonal Anti-Human Immunodeficiency Virus Type 1 (HIV-1) p24 Gag protein, Clone AG3.0 (produced *in vitro*), HRP-20068, contributed by Creative Biolabs.

**Author contributions:** JG, CAE, and KLJS contributed study conceptualization and methodology. JG, JP, SS, EB, JS contributed experimental design, data acquisition, and data analysis. JG contributed original draft preparation. All authors contributed to writing, review, and editing. JG, PJG, CAE, and KJS contributed funding. All authors have read and agreed to the submitted version of the manuscript.

**Data availability statement:** All sequencing data are available in the NCBI GEO database (https://www.ncbi.nlm.nih.gov/geo/) with the accession number GSE143685. Other data used and/or analyzed during the current study are available from the corresponding author on reasonable request.

**Funding:** This research was funded by the National Institutes of Health grant no. T32 (JG), F31 MH131486(JG) , R01DA057337(PJG), R61DA058501 (PJG), R21MH129193 (CAE), R01DA049514 and R01DA052826 (KLJS), and P30AI045008 (KJS, CAE).

**Bibliography:**


1. Saylor D, Dickens AM, Sacktor N, et al. HIV-associated neurocognitive disorder - Pathogenesis and prospects for treatment. *Nat Rev Neurol*. 2016;12(4):234-248. doi:10.1038/nrneurol.2016.27
2. Li Z, Purcell DW, Sansom SL, Hayes D, Hall ; H Irene. *Vital Signs: HIV Transmission Along the Continuum of Care — United States, 2016*. https://www.cdc.gov/mmwr
3. Dash PK, Kevadiya BD, Su H, Banoub MG, Gendelman HE. Pathways towards human immunodeficiency virus elimination. *EBioMedicine*. 2020;53:102667. doi:10.1016/j.ebiom.2020.102667
4. Nakanjako D, Nabatanzi R, Ssinabulya I, et al. Chronic immune activation and accelerated immune aging among HIV-infected adults receiving suppressive antiretroviral therapy for at least 12 years in an African cohort. *Heliyon*. 2024;10(11). doi:10.1016/j.heliyon.2024.e31910
5. Kettelhut A, Bowman E, Funderburg NT. Immunomodulatory and Anti-Inflammatory Strategies to Reduce Comorbidity Risk in People with HIV. *Curr HIV/AIDS Rep*.*Springer*. 2020;17(4):394-404. doi:10.1007/s11904-020-00509-y
6. Zenebe Y, Necho M, Yimam W, Akele B. Worldwide Occurrence of HIV-Associated Neurocognitive Disorders and Its Associated Factors: A Systematic Review and Meta-Analysis. *Front Psychiatry*.*Frontiers Media S.A.* 2022;13. doi:10.3389/fpsyt.2022.814362
7. Nyamayaro P, Gouse H, Hakim J, Robbins RN, Chibanda D. Neurocognitive impairment in treatment-experienced adults living with HIV attending primary care clinics in Zimbabwe. *BMC Infect Dis*. 2020;20(1). doi:10.1186/s12879-020-05090-8
8. Nightingale S, Ances B, Cinque P, et al. Cognitive impairment in people living with HIV: consensus recommendations for a new approach. *Nat Rev Neurol*. 2023;19(7):424-433. doi:10.1038/s41582-023-00813-2
9. Williams ME, Naudé PJW. The relationship between HIV-1 neuroinflammation, neurocognitive impairment and encephalitis pathology: A systematic review of studies investigating post-mortem brain tissue. *Rev Med Virol*.*John Wiley and Sons Ltd*. 2024;34(1). doi:10.1002/rmv.2519
10. Álvarez S, Brañas F, Sánchez-Conde M, Moreno S, de Quirós JCLB, Muñoz-Fernández MÁ. Frailty, markers of immune activation and oxidative stress in HIV infected elderly. *PLoS One*. 2020;15(3). doi:10.1371/journal.pone.0230339
11. Marconi VC, Moser C, Gavegnano C, et al. Randomized Trial of Ruxolitinib in Antiretroviral-Treated Adults With Human Immunodeficiency Virus. *Clinical Infectious Diseases*. 2022;74(1):95-104. doi:10.1093/cid/ciab212

12. Wadley AL, Hendry LM, Kamerman PR, et al. Role of TNF block genetic variants in HIV-associated sensory neuropathy in black Southern Africans. *European Journal of Human Genetics*. 2015;23(3):363-368. doi:10.1038/ejhg.2014.104
13. Tavasoli A, Gelman BB, Marra CM, et al. Increasing Neuroinflammation Relates to Increasing Neurodegeneration in People with HIV. *Viruses*. 2023;15(9). doi:10.3390/v15091835
14. Ripamonti E, Gisslén M, Hagberg L, et al. Cerebrospinal fluid biomarkers associated with neurofilament light levels: A study in HIV disease. *J Neuroimmunol*. 2025;400. doi:10.1016/j.jneuroim.2025.578521
15. Sacktor N, Miyahara S, Deng L, et al. *Minocycline Treatment for HIV-Associated Cognitive Impairment Results from a Randomized Trial On Behalf of the ACTG A5235 Team*. Vol 77.; 2011.
16. Veenstra M, León-Rivera R, Li M, Gama L, Clements JE, Berman JW. Mechanisms of CNS viral seeding by HIV+ CD14+ CD16+ monocytes: Establishment and reseeding of viral reservoirs contributing to HIV-associated neurocognitive disorders. *mBio*. 2017;8(5):1-15. doi:10.1128/mBio.01280-17
17. León-Rivera R, Morsey B, Niu M, Fox HS, Berman JW. Interactions of monocytes, HIV, and art identified by an innovative scrnaseq pipeline: Pathways to reservoirs and HIV-associated comorbidities. *mBio*. 2020;11(4):1-23. doi:10.1128/mBio.01037-20
18. Elizaldi SR, Verma A, Ma ZM, et al. Deep analysis of CD4 T cells in the rhesus CNS during SIV infection. *PLoS Pathog*. 2023;19(12). doi:10.1371/journal.ppat.1011844
19. Tang Y, Chaillon A, Gianella S, et al. Brain microglia serve as a persistent HIV reservoir despite durable antiretroviral therapy. *Journal of Clinical Investigation*. 2023;133(12). doi:10.1172/JCI167417
20. Ellis RJ, Marquine MJ, Kaul M, Fields JA, Schlachetzki JCM. Mechanisms underlying HIV-associated cognitive impairment and emerging therapies for its management. *Nat Rev Neurol.Nature Research*. 2023;19(11):668-687. doi:10.1038/s41582-023-00879-y
21. Wallet C, De Rovere M, Van Assche J, et al. Microglial Cells: The Main HIV-1 Reservoir in the Brain. *Front Cell Infect Microbiol*. 2019;9(October):1-18. doi:10.3389/fcimb.2019.00362
22. Thompson KA, Cherry CL, Bell JE, McLean CA. Brain cell reservoirs of latent virus in presymptomatic HIV-infected individuals. *American Journal of Pathology*. 2011;179(4):1623-1629. doi:10.1016/j.ajpath.2011.06.039
23. Suzuki K, Zaunders J, Gates TM, et al. Elevation of cell-associated HIV-1 transcripts in CSF CD4+ T cells, despite effective antiretroviral therapy, is linked to brain injury. *Proc Natl Acad Sci U S A*. 2022;119(48). doi:10.1073/pnas.2210584119
24. Spudich S, Robertson KR, Bosch RJ, et al. Persistent HIV-infected cells in cerebrospinal fluid are associated with poorer neurocognitive

performance. *Journal of Clinical Investigation*. 2019;129(8):3339-3346. doi:10.1172/JCI127413
25. DeMarino C, Denniss J, Cowen M, et al. HIV-1 RNA in extracellular vesicles is associated with neurocognitive outcomes. *Nat Commun*. 2024;15(1). doi:10.1038/s41467-024-48644-z
26. Schlachetzki JCM, Gianella S, Ouyang Z, et al. Gene expression and chromatin conformation of microglia in virally suppressed people with HIV. *Life Sci Alliance*. 2024;7(10). doi:10.26508/lsa.202402736
27. Serramía MJ, Muñoz-Fernández MÁ, Álvarez S. HIV-1 increases TLR responses in human primary astrocytes. *Sci Rep*. 2015;5. doi:10.1038/srep17887
28. Malik S, Valdebenito S, D'Amico D, Prideaux B, Eugenin EA. HIV infection of astrocytes compromises inter-organelle interactions and inositol phosphate metabolism: A potential mechanism of bystander damage and viral reservoir survival. *Prog Neurobiol*. 2021;206. doi:10.1016/j.pneurobio.2021.102157
29. Valdebenito S, Castellano P, Ajasin D, Eugenin EA. Astrocytes are HIV reservoirs in the brain: A cell type with poor HIV infectivity and replication but efficient cell-to-cell viral transfer. *J Neurochem*. 2021;158(2):429-443. doi:10.1111/jnc.15336
30. Ko A, Kang G, Hattler JB, et al. Macrophages but not Astrocytes Harbor HIV DNA in the Brains of HIV-1-Infected Aviremic Individuals on Suppressive Antiretroviral Therapy. *Journal of Neuroimmune Pharmacology*. 2019;14(1):110-119. doi:10.1007/s11481-018-9809-2
31. Bozzelli PL, Yin T, Avdoshina V, Mocchetti I, Conant KE, Maguire-Zeiss KA. HIV-1 Tat promotes astrocytic release of CCL2 through MMP/PAR-1 signaling. *Glia*. 2019;67(9):1719-1729. doi:10.1002/glia.23642
32. Carey SD, Conant K, Maguire-Zeiss KA. Short-term exposure to HIV Tat induces glial activation and changes in perineuronal nets. *European Journal of Neuroscience*. 2024;60(3):4303-4316. doi:10.1111/ejn.16427
33. Gosselin D, Skola D, Coufal NG, et al. An environment-dependent transcriptional network specifies human microglia identity. *Science (1979)*. 2017;356(6344):1248-1259. doi:10.1126/science.aal3222
34. Somers A, Jean JC, Sommer CA, et al. Generation of transgene-free lung disease-specific human induced pluripotent stem cells using a single excisable lentiviral stem cell cassette. *Stem Cells*. 2010;28(10):1728-1740. doi:10.1002/stem.495
35. Gandre-Babbe S, Paluru P, Aribeana C, et al. Patient-derived induced pluripotent stem cells recapitulate hematopoietic abnormalities of juvenile myelomonocytic leukemia. *Blood*. 2013;121(24):4925-4929. doi:10.1182/blood-2013-01-478412
36. Ryan SK, Gonzalez M V., Garifallou JP, et al. Neuroinflammation and EIF2 Signaling Persist despite Antiretroviral Treatment in an hiPSC Tri-culture Model of HIV Infection. *Stem Cell Reports*. 2020;14(4):703-716. doi:10.1016/j.stemcr.2020.02.010

37. O'Donnell LA, Agrawal A, Jordan-Sciutto KL, Dichter MA, Lynch DR, Kolson DL. Human immunodeficiency virus (HIV)-induced neurotoxicity: Roles for the NMDA receptor subtypes 2A and 2B and the calcium-activated protease calpain by a CSF-derived HIV-1 strain. *Journal of Neuroscience*. 2006;26(3):981-990. doi:10.1523/JNEUROSCI.4617-05.2006
38. Zhai J, Traebert M, Zimmermann K, et al. Comparative study for the IMI2-NeuroDeRisk project on microelectrode arrays to derisk drug-induced seizure liability. *J Pharmacol Toxicol Methods*. 2023;123. doi:10.1016/j.vascn.2023.107297
39. Chen W, Sulcove J, Frank I, Jaffer S, Ozdener H, Kolson DL. Development of a Human Neuronal Cell Model for Human Immunodeficiency Virus (HIV)-Infected Macrophage-Induced Neurotoxicity: Apoptosis Induced by HIV Type 1 Primary Isolates and Evidence for Involvement of the Bcl-2/Bcl-xL-Sensitive Intrinsic Apoptosis Pathway. *J Virol*. 2002;76(18):9407-9419. doi:10.1128/jvi.76.18.9407-9419.2002
40. Matt SM, Nolan R, Manikandan S, et al. Dopamine-driven increase in IL-1β in myeloid cells is mediated by differential dopamine receptor expression and exacerbated by HIV. *Journal of Neuroinflammation* . 2025;22(1). doi:10.1186/s12974-025-03403-9
41. Conesa A, Madrigal P, Tarazona S, et al. A survey of best practices for RNA-seq data analysis. *Genome Biol.BioMed Central Ltd.* 2016;17(1). doi:10.1186/s13059-016-0881-8
42. Hänzelmann S, Castelo R, Guinney J. *GSVA: Gene Set Variation Analysis for Microarray and RNA-Seq Data*. Vol 14.; 2013. http://www.biomedcentral.com/1471-2105/14/7http://www.bioconductor.org.Background
43. *Application Notes Advertising Feature*.; 2008. http://www.nature.com/naturemethods
44. Lord SJ, Velle KB, Dyche Mullins R, Fritz-Laylin LK. SuperPlots: Communicating reproducibility and variability in cell biology. *Journal of Cell Biology*.*Rockefeller University Press*. 2020;219(6). doi:10.1083/JCB.202001064
45. Fixsen BR, Han CZ, Zhou Y, et al. SALL1 enforces microglia-specific DNA binding and function of SMADs to establish microglia identity. *Nat Immunol*. 2023;24(7):1188-1199. doi:10.1038/s41590-023-01528-8
46. Guo H, Gao J, Taxman DJ, Ting JPY, Su L. HIV-1 infection induces interleukin-1β production via TLR8 protein-dependent and NLRP3 inflammasome mechanisms in human monocytes. *Journal of Biological Chemistry*. 2014;289(31):21716-21726. doi:10.1074/jbc.M114.566620
47. Carvallo L, Lopez L, Fajardo JE, Jaureguiberry-Bravo M, Fiser A, Berman JW. HIV-Tat regulates macrophage gene expression in the context of neuroAIDS. *PLoS One*. 2017;12(6):1-21. doi:10.1371/journal.pone.0179882

48. Abud EM, Ramirez RN, Martinez ES, et al. iPSC-Derived Human Microglia-like Cells to Study Neurological Diseases. *Neuron*. 2017;94(2):278-293.e9. doi:10.1016/j.neuron.2017.03.042
49. Liddelow SA, Guttenplan KA, Clarke LE, et al. Neurotoxic reactive astrocytes are induced by activated microglia. *Nature*. 2017;541(7638):481-487. doi:10.1038/nature21029
50. Chun TW, Engel D, Mizell SB, Ehler LA, Fauci AS. *Induction of HIV-1 Replication in Latently Infected CD4 T Cells Using a Combination of Cytokines*. Vol 188.; 1998. http://www.jem.org
51. Larragoite ET, Nell RA, Martins LJ, Barrows LR, Planelles V, Spivak AM. Histone deacetylase inhibition reduces deleterious cytokine release induced by ingenol stimulation. *Biochem Pharmacol*. 2022;195. doi:10.1016/j.bcp.2021.114844
52. Chen J, He Y, Zhong H, et al. Transcriptome analysis of CD4+ T cells from HIV-infected individuals receiving ART with LLV revealed novel transcription factors regulating HIV-1 promoter activity. *Virol Sin*. 2023;38(3):398-408. doi:10.1016/j.virs.2023.03.001
53. Alvarez-Carbonell D, Ye F, Ramanath N, Dobrowolski C, Karn J. The Glucocorticoid Receptor Is a Critical Regulator of HIV Latency in Human Microglial Cells. *Journal of Neuroimmune Pharmacology*. 2019;14(1):94-109. doi:10.1007/s11481-018-9798-1
54. Liu T, Zhang L, Joo D, Sun SC. NF-κB signaling in inflammation. *Signal Transduct Target Ther*. Published online 2017. doi:10.1038/sigtrans.2017.23
55. Hattori SI, Matsuda K, Tsuchiya K, et al. Combination of a Latency-ReversingAgent With a Smac Mimetic Minimizes secondary HIV-1 Infection in vitro. *Front Microbiol*. 2018;9(SEP). doi:10.3389/fmicb.2018.02022
56. Lee J, Rhee MH, Kim E, Cho JY. BAY 11-7082 is a broad-spectrum inhibitor with anti-inflammatory activity against multiple targets. *Mediators Inflamm*. 2012;2012. doi:10.1155/2012/416036
57. Rosario-Rodríguez LJ, Cantres-Rosario YM, Carrasquillo-Carrión K, et al. Quantitative Proteomics Reveal That CB2R Agonist JWH-133 Downregulates NF-κB Activation, Oxidative Stress, and Lysosomal Exocytosis from HIV-Infected Macrophages. *Int J Mol Sci*. 2024;25(6). doi:10.3390/ijms25063246
58. Zenón F, Cantres-Rosario Y, Adiga R, et al. HIV-infected microglia mediate cathepsin B-induced neurotoxicity. *J Neurovirol*. 2015;21(5):544-558. doi:10.1007/s13365-015-0358-7
59. Datta G, Miller NM, Afghah Z, Geiger JD, Chen X. Hiv-1 gp120 promotes lysosomal exocytosis in human schwann cells. *Front Cell Neurosci*. 2019;13. doi:10.3389/fncel.2019.00329
60. Santerre M, Arjona SP, Allen CN, Callen S, Buch S, Sawaya BE. HIV-1 Vpr protein impairs lysosome clearance causing SNCA/alpha-synuclein accumulation in neurons. *Autophagy*. 2021;17(7):1768-1782. doi:10.1080/15548627.2021.1915641

61. Fan Y, He JJ. HIV-1 tat promotes lysosomal exocytosis in astrocytes and contributes to astrocyte-mediated tat neurotoxicity. *Journal of Biological Chemistry*. 2016;291(43):22830-22840. doi:10.1074/jbc.M116.731836
62. Gelman BB, Endsley J, Kolson D. When do models of NeuroAIDS faithfully imitate “the real thing”? *J Neurovirol.Springer*. 2018;24(2):146-155. doi:10.1007/s13365-017-0601-5
63. Chan P, Hellmuth J, Spudich S, Valcour V. Cognitive Impairment and Persistent CNS Injury in Treated HIV. *Curr HIV/AIDS Rep.Current Medicine Group LLC 1*. 2016;13(4):209-217. doi:10.1007/s11904-016-0319-7
64. Singh K, Natarajan V, Dewar R, et al. Long-Term persistence of transcriptionally active “defective” HIV-1 proviruses: Implications for persistent immune activation during antiretroviral therapy. *AIDS*. 2023;37(14):2119-2130. doi:10.1097/QAD.0000000000003667
65. Byrnes SJ, Busman-Sahay K, Angelovich TA, et al. Chronic immune activation and gut barrier dysfunction is associated with neuroinflammation in ART-suppressed SIV+ rhesus macaques. *PLoS Pathog*. 2023;19(3). doi:10.1371/journal.ppat.1011290
66. Kilroy JM, Leal AA, Henderson AJ. Chronic HIV Transcription, Translation, and Persistent Inflammation. *Viruses.Multidisciplinary Digital Publishing Institute (MDPI)*. 2024;16(5). doi:10.3390/v16050751
67. Liu WL, Lin HW, Lin MR, et al. Emerging blood exosome-based biomarkers for preclinical and clinical Alzheimer’s disease: A meta-Analysis and systematic review. *Neural Regen Res.Wolters Kluwer Medknow Publications*. 2022;17(11):2381-2390. doi:10.4103/1673-5374.335832
68. Norris JG, Tang LP, Sparacio SM, Benveniste EN. *Signal Transduction Pathways Mediating Astrocyte IL-6 Induction by IL-Lp and Tumor Necrosis Factor-a’*.; 1994. http://www.jimmunol.org/
69. Shalaby MR, Waage A, Espevik T. Cytokine regulation of interleukin 6 production by human endothelial cells. *Cell Immunol*. 1989;121(2):372-382. doi:10.1016/0008-8749(89)90036-1
70. Perez-Valero I, Ellis R, Heaton R, et al. Cerebrospinal fluid viral escape in aviremic HIV-infected patients receiving antiretroviral therapy: Prevalence, risk factors and neurocognitive effects. *AIDS*. 2019;33(3):475-481. doi:10.1097/QAD.0000000000002074
71. Kincer LP, Dravid A, Trunfio M, et al. Neurosymptomatic HIV-1 CSF escape is associated with replication in CNS T cells and inflammation. *J Clin Invest*. 2024;134(19). doi:10.1172/JCI176358
72. Guha D, Misra V, Yin J, Gabuzda D. CSF Inflammation Markers Associated with Asymptomatic Viral Escape in Cerebrospinal Fluid of HIV-Positive Individuals on Antiretroviral Therapy. *Viruses*. 2023;15(9). doi:10.3390/v15091829
73. Alvarez-Carbonell D, Ye F, Ramanath N, et al. Cross-talk between microglia and neurons regulates HIV latency. *PLoS Pathog*. 2019;15(12). doi:10.1371/JOURNAL.PPAT.1008249

74. Sreeram S, Ye F, Garcia-Mesa Y, et al. The potential role of HIV-1 latency in promoting neuroinflammation and HIV-1-associated neurocognitive disorder. *Trends Immunol*.*Elsevier Ltd*. 2022;43(8):630-639. doi:10.1016/j.it.2022.06.003

a.

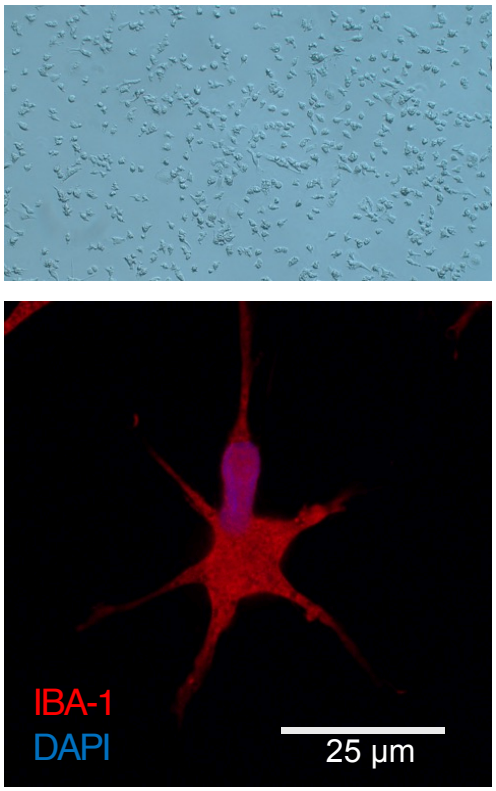


b.

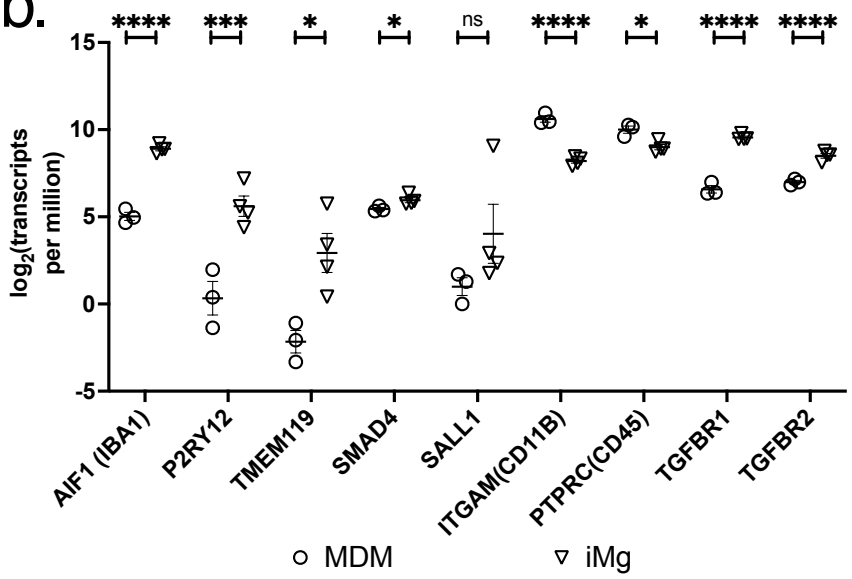


c.

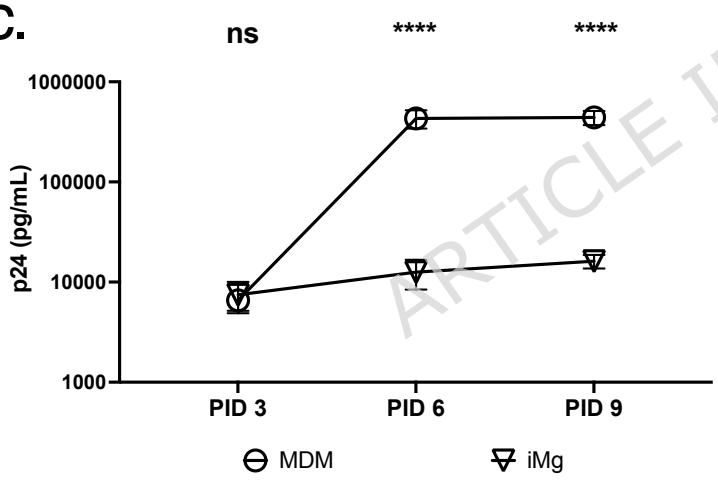


d.

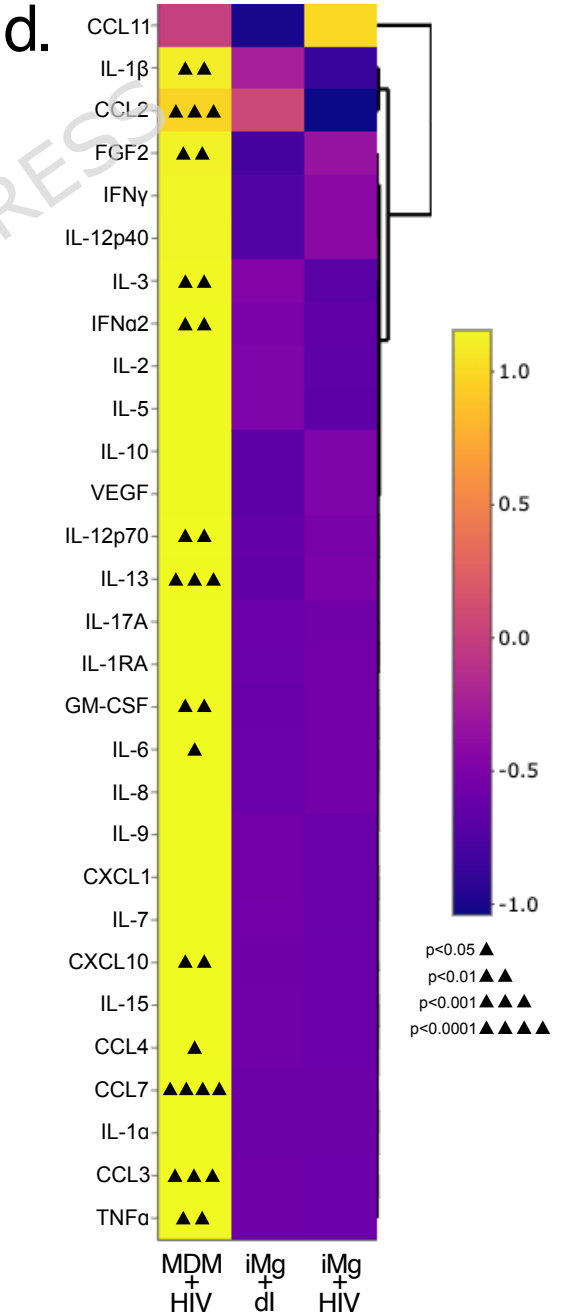


e.

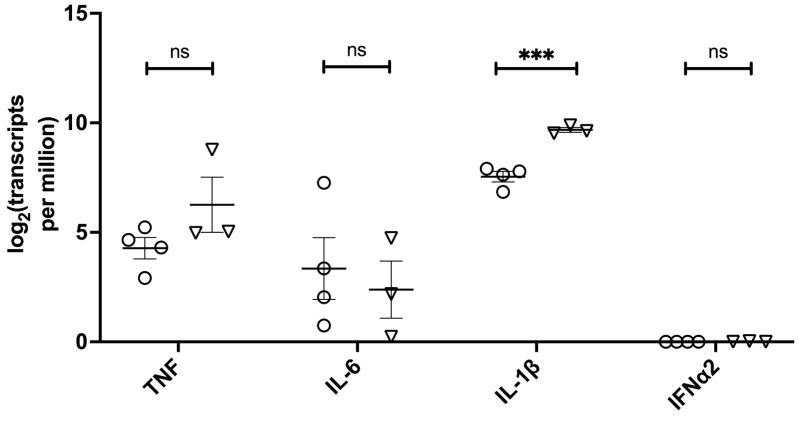


**Figure 1**

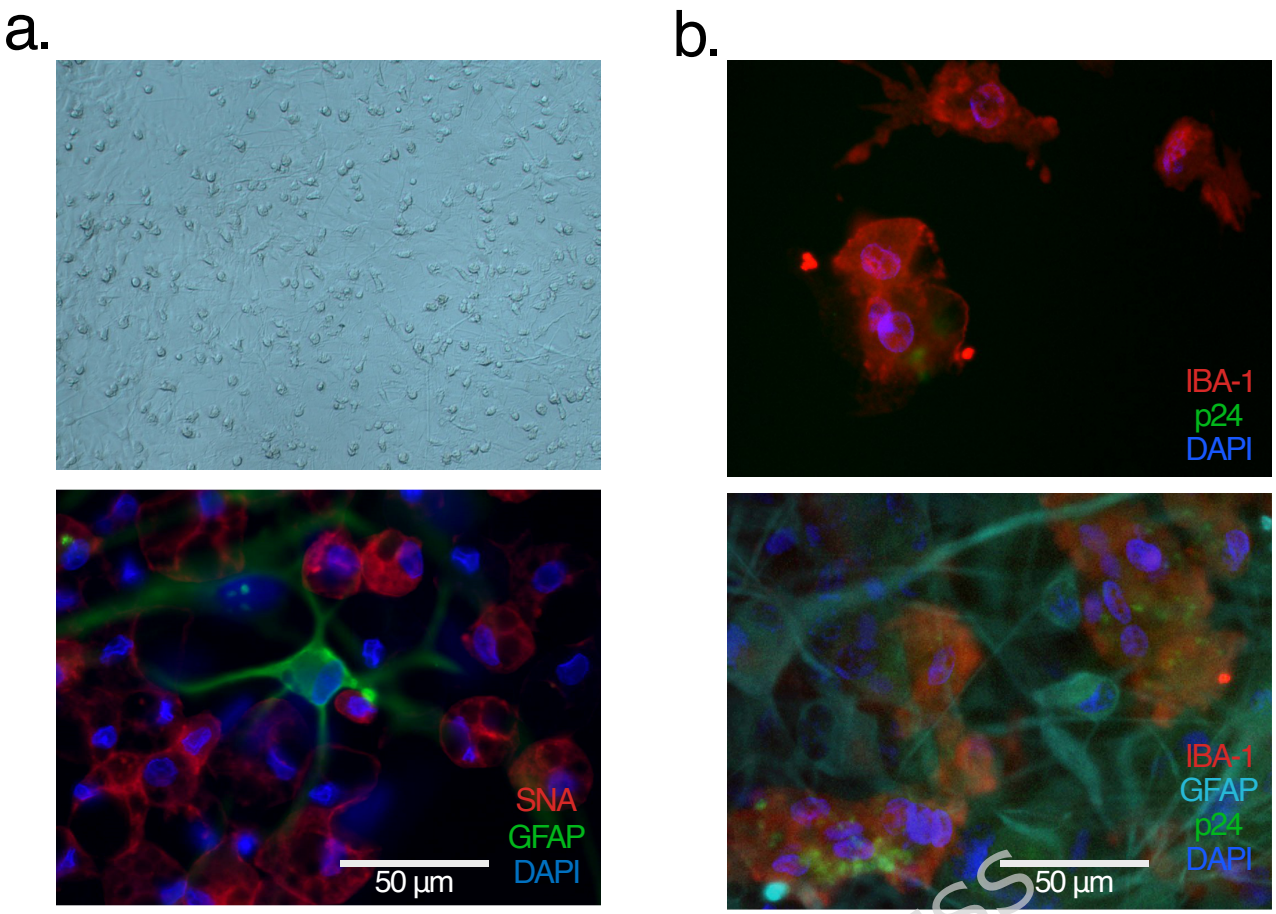




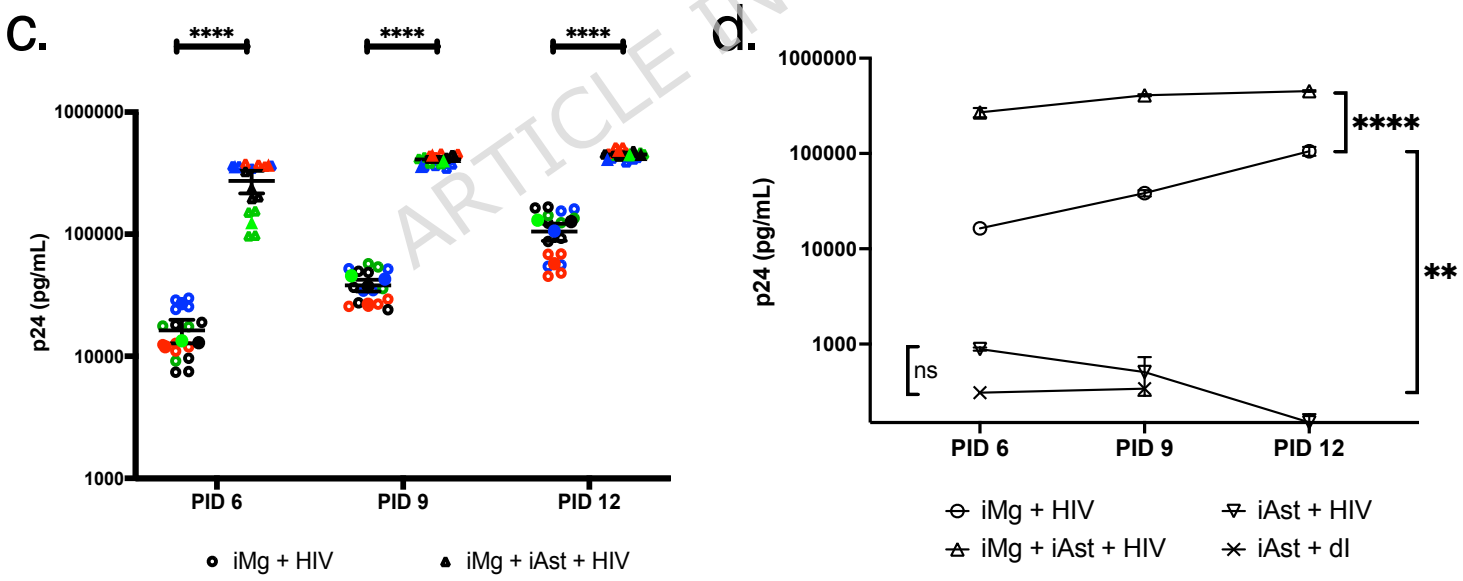


**Figure 2**

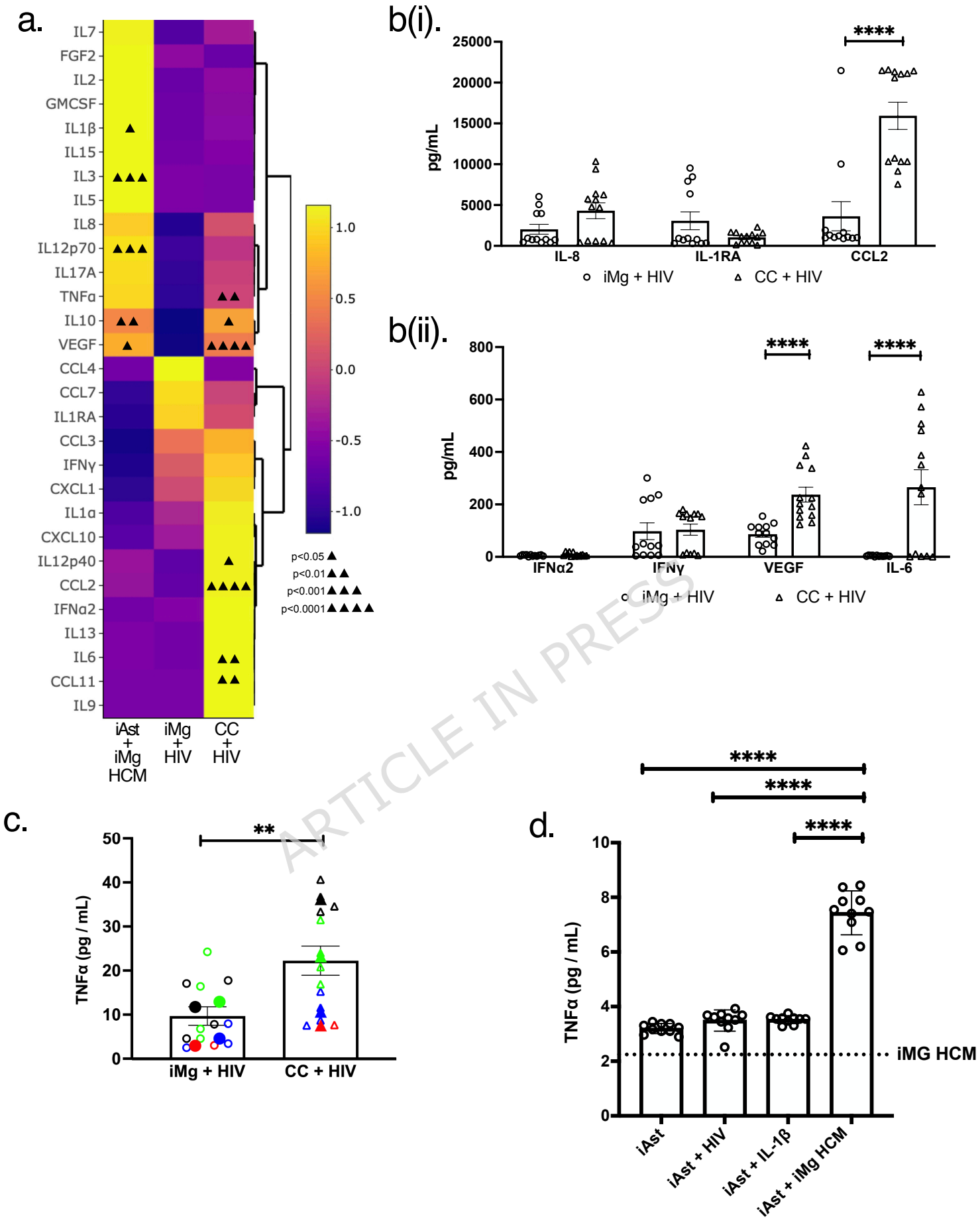




**Figure 3**

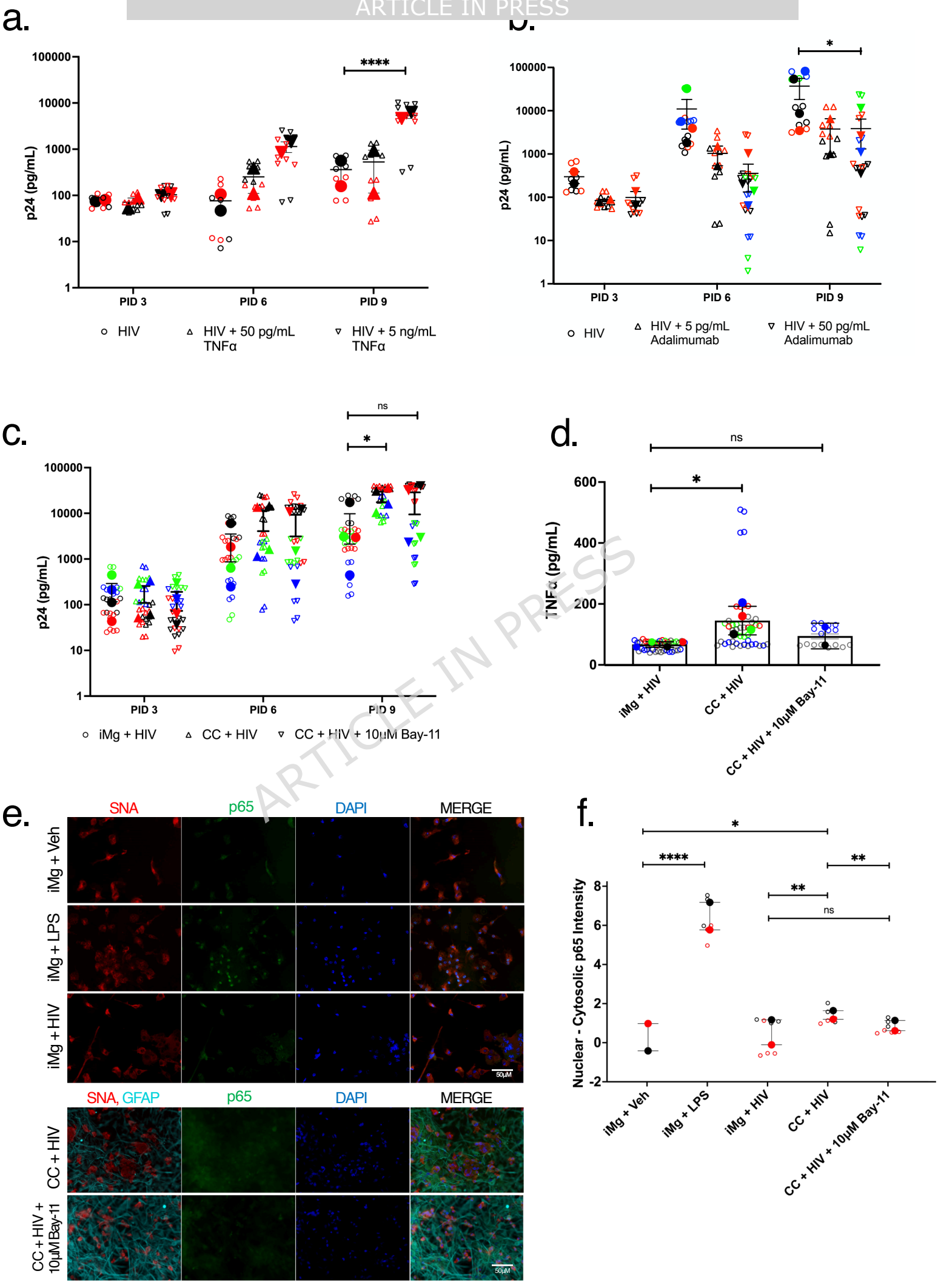


**Figure 4**

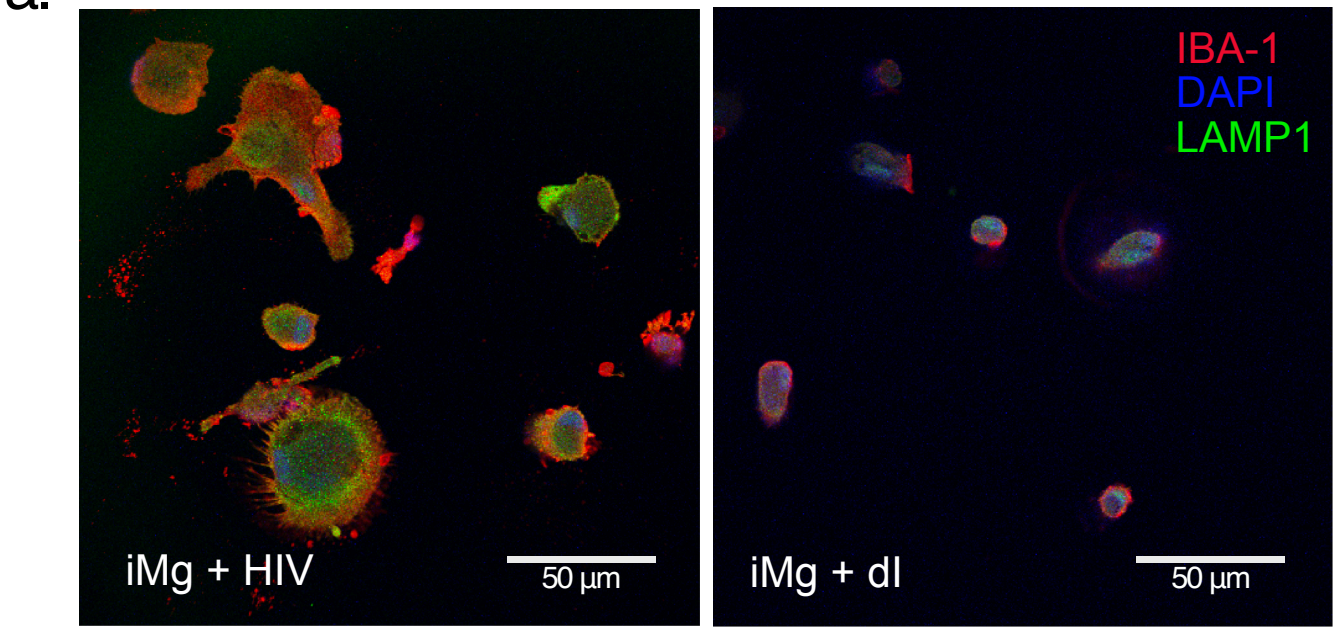


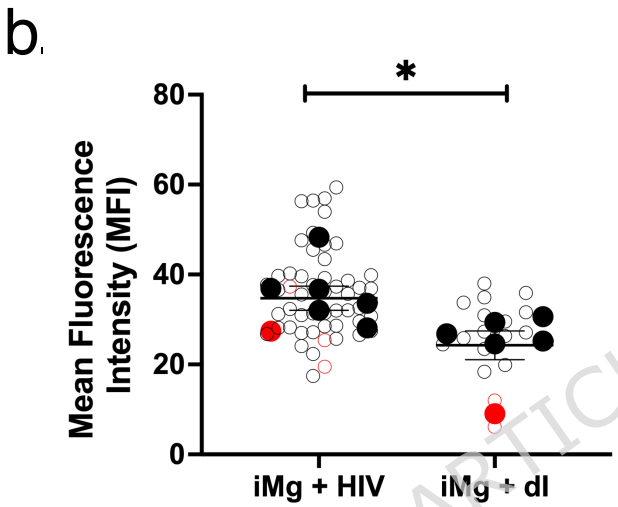


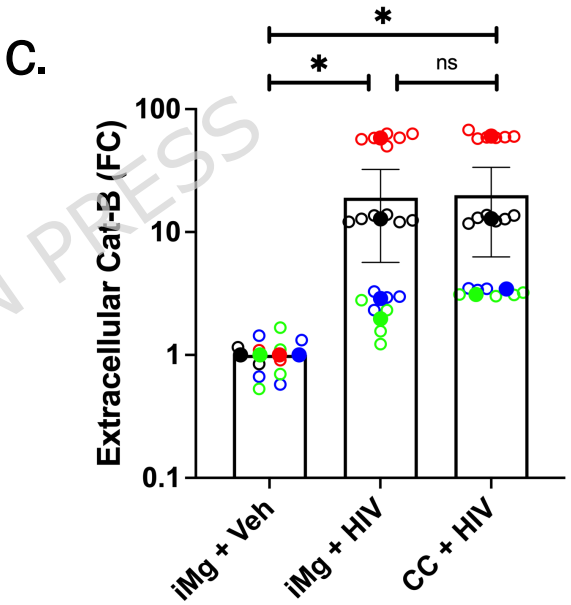




**Figure 5**

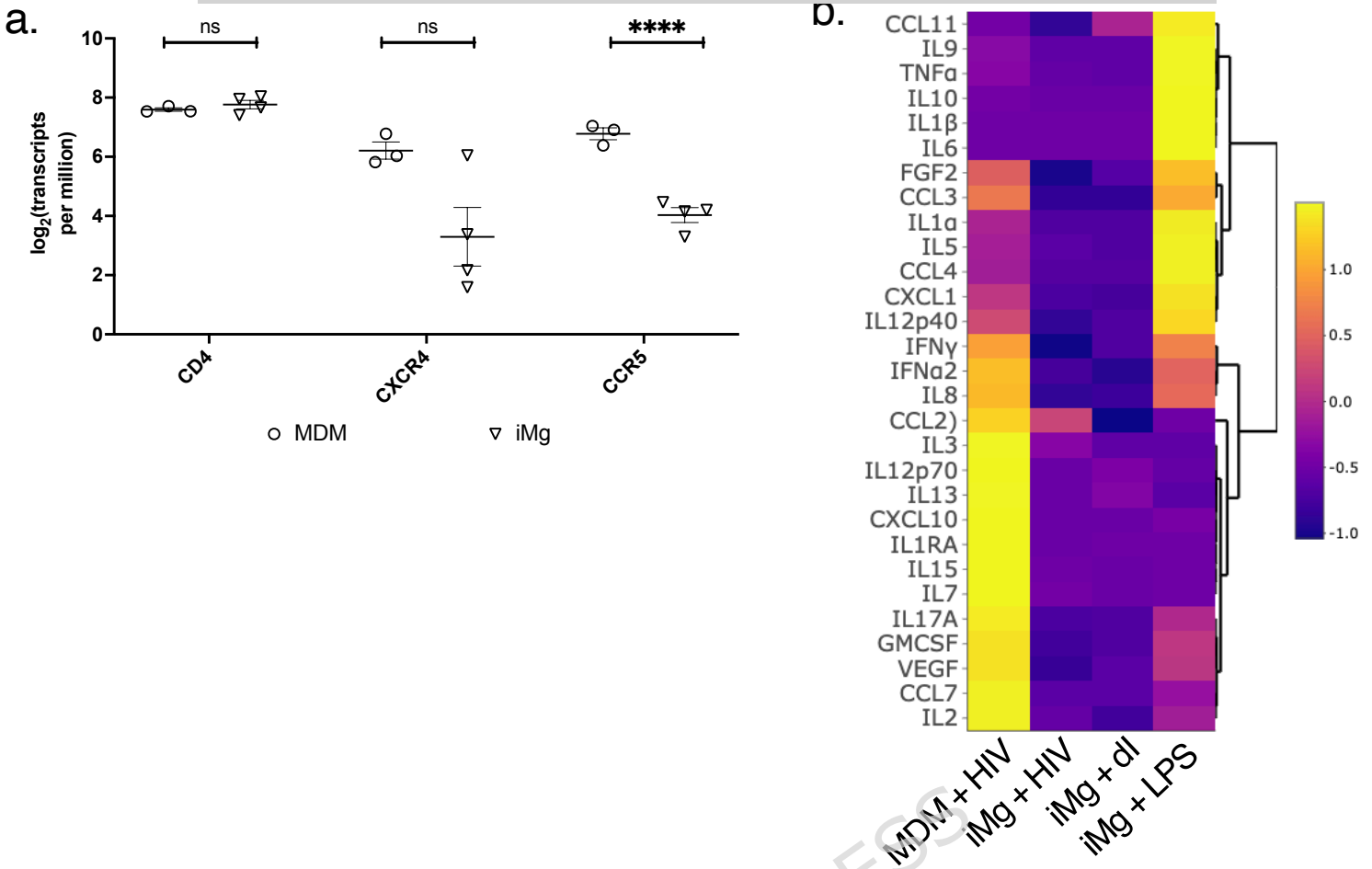




**Supplementary Figure 1**

a.

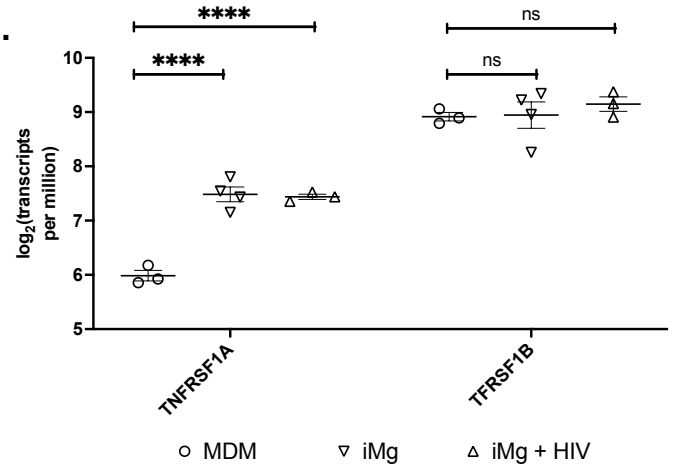




**Supplementary Figure 2**

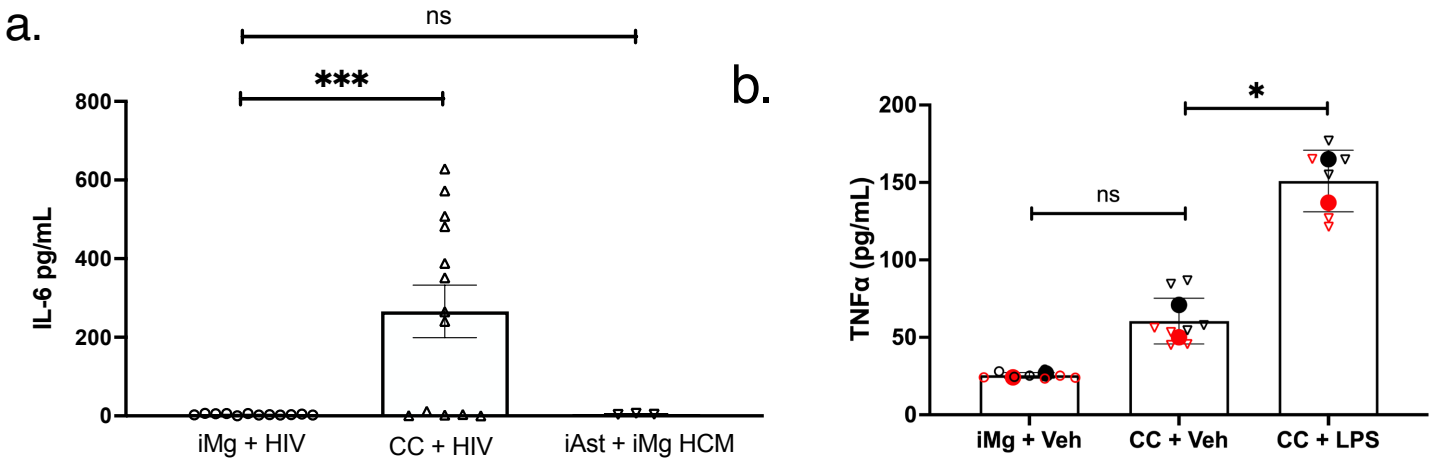




**Supplementary Figure 3**

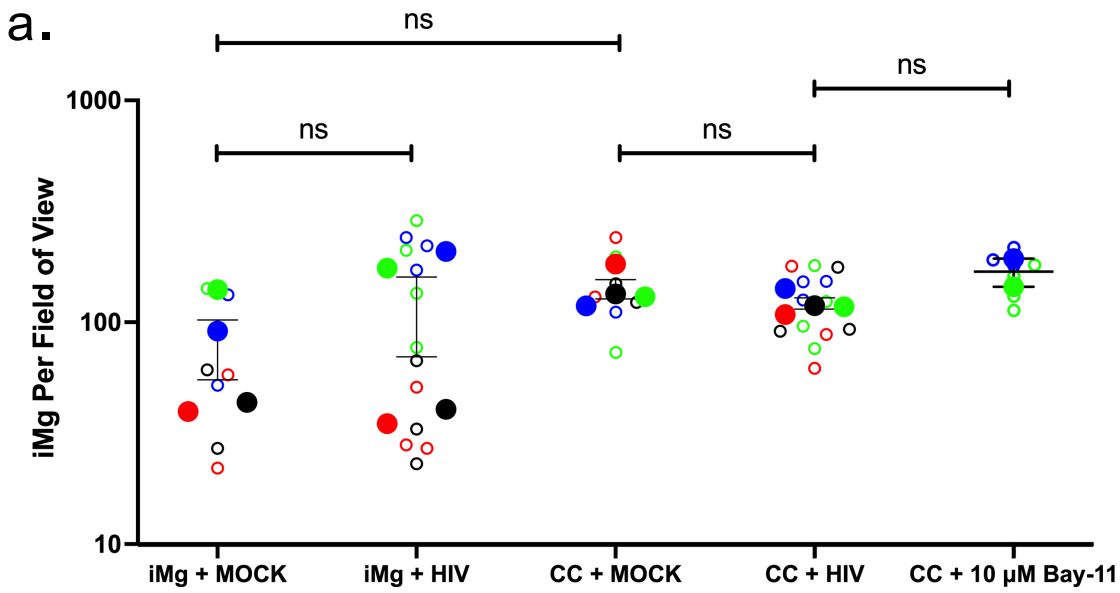




**Supplementary Figure 4**

a.

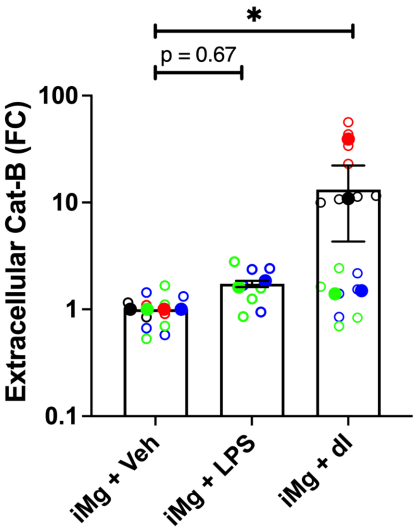




**Supplementary Figure 5**